Geoscience Frontiers 5 (2014) 369–394

Contents lists available at ScienceDirect

China University of Geosciences (Beijing)

Geoscience Frontiers

journal homepage: www.elsevier.com/locate/gsf

Focus paper

The Emeishan large igneous province: A synthesis

J. Gregory Shellnutt*

National Taiwan Normal University, Department of Earth Science, 88 Tingzhou Road Section 4, Taipei 11677, Taiwan

ARTICLE INFO

Article history:
Received 9 April 2013
Received in revised form
16 July 2013
Accepted 20 July 2013
Available online 7 August 2013

Keywords:
Late Permian
Mantle plume
Large igneous province
Flood basalts
Mineral deposits
Uplift and doming

ABSTRACT

The late Permian Emeishan large igneous province (ELIP) covers $\sim 0.3 \times 10^6$ km^2 of the western margin of the Yangtze Block and Tibetan Plateau with displaced, correlative units in northern Vietnam (Song Da zone). The ELIP is of particular interest because it contains numerous world-class base metal deposits and is contemporaneous with the late Capitanian ($\sim$260 Ma) mass extinction. The flood basalts are the signature feature of the ELIP but there are also ultramafic and silicic volcanic rocks and layered mafic-ultramafic and silicic plutonic rocks exposed. The ELIP is divided into three nearly concentric zones (i.e. inner, middle and outer) which correspond to progressively thicker crust from the inner to the outer zone. The eruptive age of the ELIP is constrained by geological, paleomagnetic and geochronological evidence to an interval of $\leq$3 Ma. The presence of picritic rocks and thick piles of flood basalts testifies to high temperature thermal regime however there is uncertainty as to whether these magmas were derived from the subcontinental lithospheric mantle or sub-lithospheric mantle (i.e. asthenosphere or mantle plume) sources or both. The range of Sr ($I_{Sr} \approx 0.7040$–0.7132), Nd ($\varepsilon_{Nd}(t) \approx -14$ to $+8$), Pb ($^{206}Pb/^{204}Pb_1 \approx 17.9$–$20.6$) and Os ($\gamma_{Os} \approx -5$ to $+11$) isotope values of the ultramafic and mafic rocks does not permit a conclusive answer to ultimate source origin of the primitive rocks but it is clear that some rocks were affected by crustal contamination and the presence of near-depleted isotope compositions suggests that there is a sub-lithospheric mantle component in the system. The silicic rocks are derived by basaltic magmas/rocks through fractional crystallization or partial melting, crustal melting or by interactions between mafic and crustal melts. The formation of the Fe-Ti-V oxide-ore deposits is probably due to a combination of fractional crystallization of Ti-rich basalt and fluxing of CO_2-rich fluids whereas the Ni-Cu-(PGE) deposits are related to crystallization and crustal contamination of mafic or ultramafic magmas with subsequent segregation of a sulphide-rich portion. The ELIP is considered to be a mantle plume-derived LIP however the primary evidence for such a model is less convincing (e.g. uplift and geochemistry) and is far more complicated than previously suggested but is likely to be derived from a relatively short-lived, plume-like upwelling of mantle-derived magmas. The emplacement of the ELIP may have adversely affected the short-term environmental conditions and contributed to the decline in biota during the late Capitanian.

1. Introduction

The study of mafic continental large igneous provinces (LIPs) requires the application of a broad range of disciplines within the earth and biological sciences to explain the physical transfer of material from the mantle to the crust and its effect on the biosphere. In the broadest sense continental mafic LIPs are large (i.e. $>0.5 \times 10^5$ km^2) spatially contiguous regions of the continental crust which host temporally and petrogenetically associated igneous rocks predominated by mafic compositions (Sheth, 2007a). The formation of LIPs is debated as some are considered to be derived by deep-seated diapiric upwellings of high temperature magmas (i.e. mantle plume) whereas others are considered to be derived by relatively shallow mantle melting associated with tensile stress in the overriding lithosphere (Jerram and Widdowson, 2005; Campbell, 2007; Saunders et al., 2007; Bryan and Ernst, 2008; Foulger, 2010). Regardless of their formation, LIPs are

* Tel.: +886 2 7734 6386; fax: +886 2 2933 3315.
E-mail addresses: jgshelln@ntnu.edu.tw, gshellnutt@hotmail.com.

Peer-review under responsibility of China University of Geosciences (Beijing)

Production and hosting by Elsevier

1674-9871/$ – see front matter © 2013, China University of Geosciences (Beijing) and Peking University. Production and hosting by Elsevier B.V. All rights reserved.
http://dx.doi.org/10.1016/j.gsf.2013.07.003

either directly or indirectly a consequence of plate tectonics and the cooling of the Earth (Wilson, 1963; Morgan, 1971, 1972; White and McKenzie, 1989, 1995; Coffin and Eldholm, 1994; Ernst and Buchan, 2003).

The emplacement and eruption of LIP magmas are often coincident with mass extinctions as four of the major (i.e. Cretaceous–Paleogene, Triassic–Jurassic, middle Permian and Permian–Triassic) mass extinctions are contemporaneous with the formation of the Deccan Traps, Central Atlantic Magmatic Province, Emeishan large igneous province and the Siberia Traps (Raup and Sepkoski, 1982; Rampino and Stothers, 1988; Courtillot et al., 1999; Wignall, 2001, 2005; Courtillot and Renne, 2003; White and Saunders, 2005; Wignall et al., 2009). The emission of particulate and gasses (i.e. SO_2 and CO_2) from the erupting lavas as well as country rock degassing may be sufficient to induce climate change, cause a reduction in sunlight and inhibit photosynthesis and/or induce acid rain (Wignall, 2001; Ganino and Arndt, 2009). However not all LIPs are coincident with biotic crises and therefore the relationship may not be clear-cut (Courtillot and Renne, 2003; Shellnutt et al., 2011a). Although LIPs may contribute to ecosystem collapse they are also important sites for economic deposits of precious and base metals (Pirajno, 2000; Borisenko et al., 2006; Ernst, 2007; Zhang et al., 2008a, b). In many cases the ore deposits are orthomagmatic (i.e. layered intrusions, volcanogenic massive sulphide) but due to the large volume of hot magmas passing through the crust it is possible to form a variety of types including skarns and hydrothermal copper and gold.

The late Permian Emeishan large igneous province (ELIP) is relatively small compared to the Siberian Traps or Central Atlantic Magmatic Province but is the focus of a tremendous amount of geological, geochemical, paleomagnetic, geochronological and biostratigraphic research during the past three decades. In spite of its stature as a 'smaller' large igneous province, the ELIP is an important geological feature of SW China not only because it hosts a number of world-class orthomagmatic Fe-Ti-V oxide deposits and series of smaller economically important Ni-Cu-(PGE) sulphide deposits but also the eruption of the Emeishan flood basalts is contemporaneous with the late Capitanian–early Wuchiapingian mass extinction (i.e. end-Guadalupian) indicating that there may be a link between the two (Zhou et al., 2002a; Zhang et al., 2006a, b; Ganino and Arndt, 2009; Sun et al., 2010; Shellnutt et al., 2012a). Beyond the flood basalts, economic and biogeological importance, the ELIP contains a diverse set of igneous rocks including cumulate mafic-ultramafic layered intrusions, picrites and the full spectrum of volcanic and plutonic silicic rocks (i.e. andesites, trachytes, rhyolites, syenites, granites). The fact that the magmatic plumbing system of the ELIP is well exposed at the surface is relatively special because the plutonic-hypabyssal rocks are not often observed within continental mafic LIPs thus providing a nearly complete account of its development. The bulk of the geological and petrological research, including evidence of structural doming of the crust and high temperature picritic lavas, suggests that the ELIP was formed by a mantle plume. Consequently it is considered to be one of the best examples of a mantle plume-derived LIP and can be used as a benchmark for comparison with other continental mafic LIPs (Campbell, 2005).

The numerous studies have produced a general understanding on the formation of the ELIP but recently many of the old views are giving way to new ideas which challenge the conventional orthodoxy. Specifically that the ELIP shows evidence for doming of the crust or that it was derived by a mantle plume is questioned as well as the ongoing debate regarding the formation of the flood basalts and oxide-ore deposits (Song et al., 2001, 2004, 2008a; Xu et al., 2001, 2004; He et al., 2003; Zhou et al., 2005; Ganino et al., 2008; Utskins-Peate and Bryan, 2008; Sun et al., 2010; Shellnutt and Jahn, 2011; Shellnutt et al., 2011b; Zhong et al., 2011a; Kamenetsky et al., 2012). The objective of this paper is to provide an overview of the major features and issues regarding the formation of the ELIP. The paper is divided into seven parts which focus on a specific topic. The first part discusses the basic geological background of the ELIP including its context within the geology of China. The second part discusses the age and duration ELIP including the uncertainties between geochronological techniques and interpretations. The third part discusses the formation of the non-mineralized magmatic rocks. The fourth part focuses on the structural features, i.e. evidence for a fossil plume head and crust doming, and the effect that magmatism may have had on the late middle Permian ecosystem. The metallogenesis of the ELIP is the focus of the fifth part, specifically the formation of the Ni-Cu-(PGE) sulphide and the Fe-Ti-V oxide deposits as well as some thoughts on the potential formation of rare earth element (REE) deposits. The sixth section attempts to bring all of the information together outlined in the previous sections and provide a synthesis of the ELIP. The final section discusses future research directions and opinions of ELIP-related topics.

2. Geological background

China is composed of three major Precambrian blocks and smaller terranes which have been amalgamating since $\sim$1850 Ma or earlier (Fig. 1). In the east, the Archean North China Block (NCB) also known as the Sino-Korean Craton is bounded to the North by the Central Asia Orogenic Belt (CAOB), a Proterozoic to Paleozoic fold and thrust belt, and to the South by the middle Triassic Central Orogenic Belt (Qinling-Dabie Orogenic Belt). To the west of the NCB and the north of the Tibetan Plateau is the Tarim Block which is a Paleoproterozoic stable craton. Southeast of the Tibetan Plateau is the South China Block, a composite craton of the Yangtze Block and the Cathaysia Block (Fig. 1).

The NCB consists of two major Archean continental fragments surrounded by Paleoproterozoic orogenic belts (Zhao et al., 2005, 2006). From the late Paleoproterozoic to the Paleozoic shallow marine carbonates were deposited on many parts of the NCB. During this time, the southern margin was a site of volcanic arc accretion and granitic magmatism (1400–1000 Ma). During the Neoproterozoic extensive rift basins were formed along the northern and southern margins of the NCB (Wang and Mo, 1995; Li, 1998).

To the south of the Central Orogenic Belt is the South China Block (SCB) which comprises the Archean–Proterozoic Yangtze Block to the northwest and the Paleo-Mesoproterozoic Cathaysia Block to the southeast (Wang and Mo, 1995; Chen and Jahn, 1998). These two blocks are in contact along the Jiangshan-Shaoxing fault zone and likely collided during the late Mesoproterozoic ($\sim$1000 Ma) although this is debated (Hsu et al., 1990; Chen and Jahn, 1998). To the immediate west of the SCB is the Tibetan Plateau. The Tibetan Plateau consists of four distinct terranes, the Lhasa, Qiangtang, Yidun and Songpan-Ganze, a late Triassic–early Jurassic thrust sequence composed of 10 km thick marine sediments (Bruguier et al., 1997; Yan et al., 2003). Many of these terranes were accreted during the Paleozoic to Mesozoic and were deformed during the India-Eurasia collision (Wang and Mo, 1995; Yin and Harrison, 2000).

Southwestern China comprises the western margin of the Yangtze Block to the east and the eastern most part of the Tibetan Plateau to the west (Fig. 1). The Yangtze Block consists of Meso-Proterozoic granitic gneisses and metasedimentry rocks which have been intruded by Neoproterozoic ($\sim$800 Ma) granites and mafic rocks (Zhou et al., 2002b; Zhao and Zhou, 2007). The Neoproterozoic granites are overlain by a series of marine and

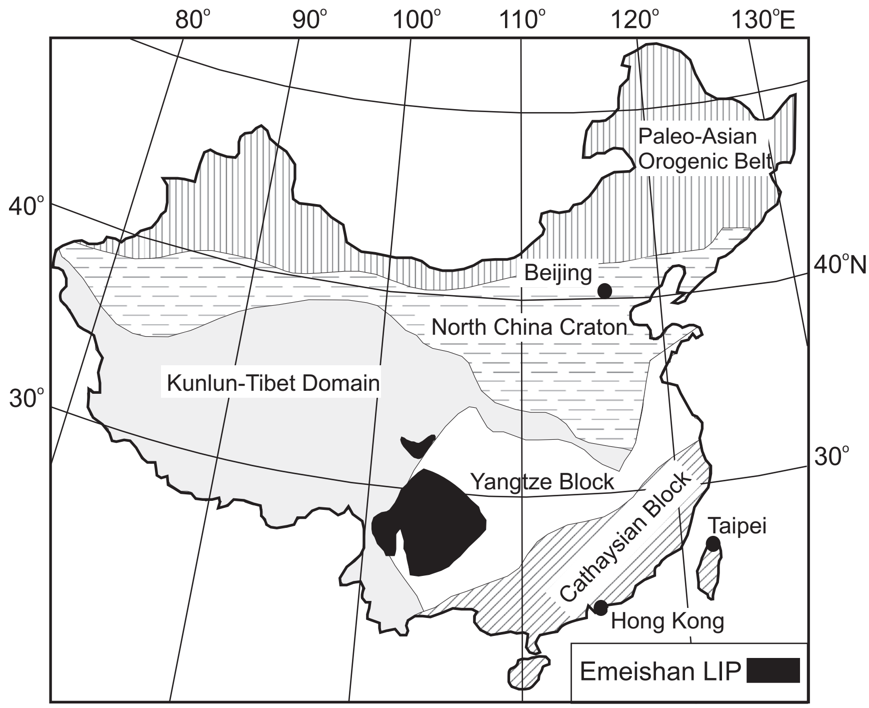

Figure 1. Major tectonic divisions of China (modified from Zhang et al., 1988).

terrestrial strata of the late Neoproterozoic (~600 Ma) to the Permian (Yan et al., 2003). The largest, single geological feature of SW China is the late Permian ELIP and is located at the western edge of the Yangtze Block near the boundary with the Songpan-Ganze terrane (Figs. 1 and 2). The wedge shape distribution of ELIP rocks is likely related to Mesozoic and Cenozoic faulting associated with the development of the Songpan-Ganze terrane and the India-Eurasia collision (Chung and Jahn, 1995; Chung et al., 1997, 1998). The ELIP covers an area of at least 0.3×10^6 km^2 of SW China and northern Vietnam (Song Da zone) and consists of mafic and ultramafic volcanic rocks, spatially associated felsic plutons and layered mafic-ultramafic intrusions, some of which host giant Fe-Ti-V oxide and Ni-Cu sulphide deposits and is subdivided into three roughly concentric zones (i.e. inner, intermediate and outer) which correspond to crustal thickness estimates and differential seismic velocity layers (Fig. 2a and b). The centre of the ELIP is known as the inner zone and has the thickest crust which progressively thins from the intermediate to outer zone (Zhong et al., 2002; Xu et al., 2004; Zhou et al., 2005). The volcanic piles range in thickness from 1.0 to 5.0 km in the western half and 0.2–2.6 km in the eastern half and consist mostly of flood basalts with picrites in the lower half and basaltic-andesites and silicic volcanic rocks in the upper half. The volcanic rocks erupted at equatorial latitudes of eastern Pangaea within one normal-polarity cycle suggesting rapid emplacement (Huang and Opdyke, 1998; Ali et al., 2002; Zheng et al., 2010). The ELIP is an important host of Ni-Cu-(PGE) sulphide and Fe-Ti-V oxide mineral deposits. In the central part, namely the Panxi region, of the ELIP there are abundant giant orthomagmatic Fe-Ti-V oxide deposits which contribute 35.2% Ti and 6.7% V of the total global production of these metals (Zhou et al., 2005). There are economic to sub-economic Ni-Cu-(PGE) and PGE deposits within the Panxi region but are also found in the outer parts of the ELIP (Song et al., 2003).

3. Age and duration of magmatism

Flood basalts have erupted regularly throughout the Earth's history on the order of about 1 every 20 million years for continents but possibly as often as 1 per 10 million if oceanic plateaux are also considered (Coffin and Eldholm, 2001; Ernst et al., 2005; Bryan and Ernst, 2008). The area and volume of a given flood basalt province is primarily dependent on the duration of volcanism, which is related to the rate of heat loss, material available to melt, and the medium (i.e. subaerial or subaqueous) into which the lavas erupt. Consequently, determining the start of magmatism is much easier than determining when it ended but most continental flood basalt provinces are active for $\leq$10 million years with some lasting up to 50 million years whether they are punctuated or continuous (Bryan and Ernst, 2008). The initiation of ELIP volcanism is well constrained by both biostratigraphic and radiometric techniques however the cessation of magmatism is unclear and continues to be debated.

The sedimentology and biostratigraphy constrains the eruption of the Emeishan flood basalts to the late middle Permian (He et al., 2007, 2010a; Sun et al., 2010). The Emeishan basalts erupted onto the middle Permian fusulinid-bearing Neomisellina-Yabeina zone of the carbonate Maokou Formation which suggests they erupted no early than 263 Ma (He et al., 2003, 2010b). The deposition of the Xuanwei formation at 257 $\pm$ 4 Ma marks the end of subaerial volcanism in the region indicating that it probably lasted for $\leq$10 million years (He et al., 2007). Paleomagnetic data collected from basalt sections at Duge, Zhijin, Ebian and Yanyuan show evidence for an early period of normal magnetic polarity followed by reverse polarity suggesting a relatively rapid (i.e. $\leq$1.5 Ma) emplacement coinciding within one normal-polarity episode thereby reducing the likely eruption duration by nearly three times (Huang and Opdyke, 1998; Thomas et al., 1998; Ali et al., 2002, 2005; Zheng et al., 2010). Furthermore, Thompson et al. (2001) and Xu et al. (2001) both noted the absence of weathered flow tops in most

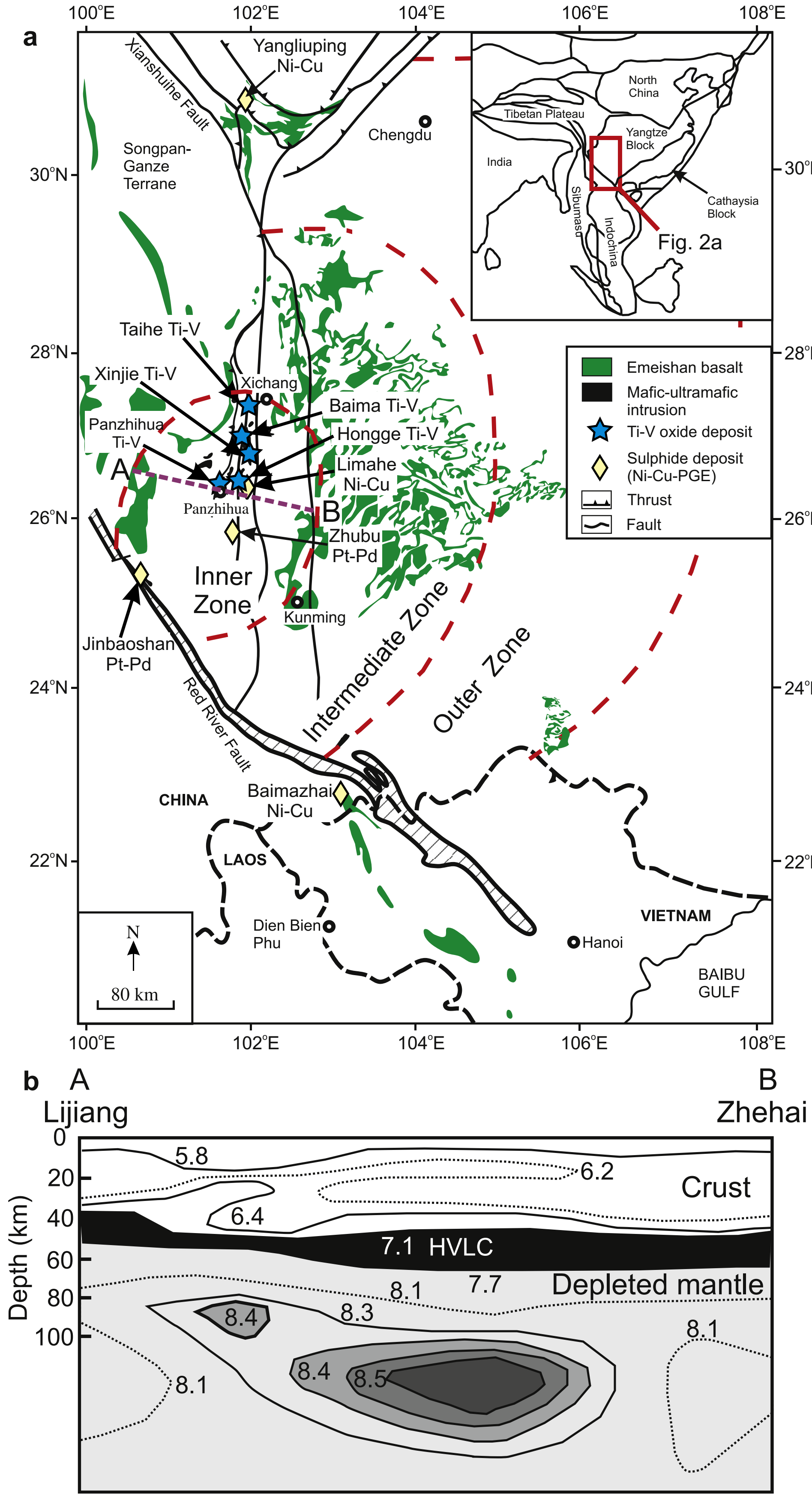

Figure 2. (a) Regional distribution of the Emeishan large igneous province showing the concentric zones (dashed red lines) of the ELIP and location of Ti-V oxide and Ni-Cu-PGE sulphide deposits (modified from Tao et al., 2010). (b) Seismic P-wave velocity (km/s) structure of the lower crust and upper mantle beneath the western Yangtze Block. The profile is from Lijiang (A) to Zhehai (B) (modified from Xu et al., 2004).

sections beneath the overlying sediments may be due to rapid emplacement and burial.

The geological and paleomagnetic data indicate that the Emeishan basalts erupted during the late middle Permian which lasted for ∼2 million years or less however the radiometric ages of all magmatic rocks reveal a more complicated situation. There are well over 50 published radiometric age dates of volcanic and plutonic rocks which are interpreted to be a part of the ELIP and range from ∼236 Ma to ∼266 Ma (Table 1). The large range of radiometric age dates for ELIP-related rocks is in direct conflict with a rapid emplacement model (Fig. 3). The range of dates may, in fact, be an artifact of different radiometric methods used, misinterpreting rocks, poor data processing and the rock type (i.e. volcanic vs. plutonic). The reported ^{40}Ar-^{39}Ar ages of the Emeishan basalts range between 246 ± 4 Ma and 256 ± 0.8 Ma and were initially interpreted to be pene-contemporaneous with the Siberian Traps and the end-Permian mass extinction. However zircon U/Pb dates of plutonic rocks consistently yielded ages around 260 Ma although there are a number of results which yielded ages between 251 Ma and 255 Ma (Fig. 3). The young ^{40}Ar-^{39}Ar basalt ages were considered to be an artifact of post-emplacement thermal resetting caused by regional tectonic events (e.g. Longmenshan thrust belt and the North China-South China collision) however, more likely, they were not corrected for systematic bias inherent in the K-Ar system that results in younger ages (Ali et al., 2004; Renne et al., 2010, 2011; Shellnutt et al., 2012a). The first high precision zircon chemical abrasion ID-TIMS geochronology results from a suite of diabase dykes and granitic rocks yielded ages tightly cluster between 257.6 ± 0.5 Ma and 259.6 ± 0.5 Ma and currently is the best emplacement age available for the ELIP (Shellnutt et al., 2012a).

The volcanic rocks likely erupted over the course of a few million (i.e. ≤2 Ma) years however that does not necessarily mean that plutonic magmatism ended as abruptly. There are many published zircon U/Pb age dates of ELIP rocks that have post-257 Ma ages and are used as evidence to suggest that plutonic magmatism continued for another 20 Ma or so (Zhong et al., 2007, 2009, 2011a; Shellnutt and Zhou, 2008; Shellnutt et al., 2008; Xu et al., 2008; Luo et al., 2013). However the relatively large (i.e. ≥2 Ma) error on some age dates does not permit greater constraint than 10 Ma and thus it cannot be verified if plutonism actually continued beyond the volcanism. Furthermore, two syenitic intrusions that were dated using the ID-TIMS methods have shown that rocks which were previously considered to be ∼252 Ma are actually ∼259 Ma and diabase dykes that were considered to be ∼242 Ma are between 257 and 259 Ma thus casting doubt on an excessively long magmatic duration (Shellnutt et al., 2012a). It is possible that plutonic magmatism continued beyond the volcanism if the heat source dissipates slowly over the course of a few million years but it is unlikely that ELIP magmatism continued for an additional 20 million years. Therefore, providing a heat source is available, it is possible that underplated mafic ELIP rocks could have served as a source for post-ELIP magmas which may have similar geochemical characteristics as the ELIP rocks (Xu et al., 2004; Shellnutt et al., 2008).

4. Magmatic rocks of the Emeishan large igneous province

Mafic continental large igneous provinces represent the physical and chemical transfer of material from the mantle to the crust (Coffin and Eldholm, 1994; Sheth, 2007a; Bryan and Ernst, 2008). The nature of the mantle melting is a debated issue and is primarily focused on whether LIPs are formed by hot, deep-seated upwelling of mantle material (i.e. mantle plume) or if they are merely formed as a consequence of shallow decompression melting in areas where the lithosphere is under extension (Richards et al., 1989; Campbell and Griffiths, 1990; Griffiths and Campbell, 1991; Sheth, 1999; Favela and Anderson, 2000; Ernst and Buchan, 2003; Campbell, 2005; Ernst et al., 2005; Natland and Winterer, 2005; Saunders et al., 2007; Bryan and Ernst, 2008; Foulger, 2010). There are a number of geological, geochemical and thermal criteria which indicate whether a given LIP is generated by a mantle plume. The main geological features associated with mantle plume-derived LIP include: short duration of magmatism (e.g. ≤1 Ma), the eruption of ultramafic lavas, thermal anomalies, voluminous flood basalts and doming of the crust (Campbell, 2007). Some of the criteria are difficult to assess, in particular the eruption duration and doming of the crust. Furthermore, determining the thermal history of an ancient LIP is problematic however it can be surmised by the presence of ultramafic lavas and by calculating their mantle potential temperatures (Herzberg and O'Hara, 2002; Herzberg et al., 2007; Herzberg and Asimow, 2008). The ELIP is considered to be a mantle plume-derived large igneous province and exhibits, to varying degrees, the criteria outlined for mantle plume-LIPs although there is evidence that the subcontinental lithospheric mantle (SCLM) may be a contributing source and that the mantle plume model is too simplistic (Song et al., 2001, 2004, 2008a; Xu et al., 2001, 2004, 2007a, b; He et al., 2003, 2007; Xiao et al., 2004; Shellnutt and Zhou, 2007; Shellnutt et al., 2008; Shellnutt and Jahn, 2011; Kamenetsky et al., 2012). This section summarizes the magmatic features of the ELIP.

4.1. *Ultramafic volcanic rocks*

High temperature ultramafic volcanic rocks are recognized within the inner zone of the ELIP at Binchaun, Yongsheng, Ertan, Muli, Dali, Jinping, and Lijiang (Polyakov et al., 1991; Glotov et al., 2001; Hanski et al., 2004, 2010; Hou et al., 2006; Zhang et al., 2006a, b; Wang et al., 2007; Ali et al., 2010; He et al., 2010c; Kamenetsky et al., 2012). There are also correlative units in the Song Da zone of northern Vietnam which was tectonically transposed by ∼600 km sinistral offset during the Paleogene activation of the Ailao Shan-Red River fault system (Chung et al., 1997). The rocks are regarded as picrites as they contain between 14 wt.% and 27 wt.% MgO but, in some cases, their composition and textures (i.e. spinifex) bear some resemblance to the komatiites of Gorgona Island (Hanski et al., 2004; Kamenetsky et al., 2012). The picrites are found at various stratigraphic levels within the volcanic piles however they are typically found no higher than the lower half which suggests they were amongst the earliest eruptive rocks (Xu et al., 2001; Hanski et al., 2004; Zhang et al., 2006a, b; Li et al., 2010).

The whole rock composition of primary mantle-derived ultramafic rocks can be used to estimate their eruption temperatures and mantle potential temperatures (McKenzie and O'Nions, 1991; Albarede, 1992; Herzberg and O'Hara, 2002; Herzberg et al., 2007; Herzberg and Asimow, 2008). The eruption and mantle potential temperatures (T_p) of the ELIP picrites have been estimated using different techniques by Xu et al. (2001), Zhang et al. (2006a, b), Ali et al. (2010) and He et al. (2010c). Xu et al. (2001), using REE inversion, have suggested that the mantle potential temperatures are >1550 °C whereas Zhang et al. (2006a, b), using the empirical estimate method of Albarede (1992), calculated a T_p of 1630–1690 °C. In contrast, both He et al. (2010c) and Ali et al. (2010) using PRIMELT2 calculated the initial MgO values of the picrites to be ≥20% which corresponds to eruption temperatures of ∼1440 °C and a mantle potential temperatures between ∼1540 °C and 1610 °C. The wide-range of estimates is perhaps a little disconcerting regarding the precision of the T_p but the fact that the temperatures are consistently >1540 °C suggests that, no matter

Table 1
Summary of reported age dates from the Emeishan large igneous province.

Sample	Rock type	Method	Material	Age (Ma)	Reference
GS03-092	Syenite	$^{206}Pb/^{238}U$	Zircon	259 ± 5	Shellnutt et al. (2009)
GS04-016	Syenite	$^{206}Pb/^{238}U$	Zircon	258 ± 4	Shellnutt et al. (2009)
GS05-056B	Gabbro	$^{206}Pb/^{238}U$	Zircon	261 ± 2	Shellnutt et al. (2009)
TH-14	Granite	$^{206}Pb/^{238}U$	Zircon	261 ± 2	Xu et al. (2008)
LQ-3	Nepheline syenite	$^{206}Pb/^{238}U$	Zircon	262 ± 4	Luo et al. (2007)
GS04-077	Mafic dyke	$^{206}Pb/^{238}U$	Zircon	261 ± 5	Shellnutt and Jahn (2011)
MY-5	Pyroxene syenite	$^{206}Pb/^{238}U$	Zircon	260 ± 4	Xu et al. (2008)
GS05-065	Syenite	$^{206}Pb/^{238}U$	Zircon	260 ± 2	Shellnutt and Zhou (2007)
HG-1	Granite	$^{206}Pb/^{238}U$	Zircon	255 ± 4	Xu et al. (2008)
ALH-0401	Granite	$^{206}Pb/^{238}U$	Zircon	251 ± 6	Zhong et al. (2007)
GS03-122	Syenite	$^{206}Pb/^{238}U$	Zircon	252 ± 3	Shellnutt and Zhou (2008)
WB-0604	Syenite	$^{206}Pb/^{238}U$	Zircon	253 ± 2	Zhong et al. (2009)
SL-2	Diorite	$^{206}Pb/^{238}U$	Zircon	260 ± 4	Xu et al. (2008)
HC-2	Quartz syenite	$^{206}Pb/^{238}U$	Zircon	266 ± 5	Xu et al. (2008)
GS04-119	Mafic dyke	$^{206}Pb/^{238}U$	Zircon	242 ± 2	Shellnutt et al. (2008)
Panzhihua	Picritic dyke	$^{206}Pb/^{238}U$	Zircon	261.4 ± 4.6	Hou et al. (2013)
BC-Tu#-3	Rhyolitic tuff	$^{206}Pb/^{238}U$	Zircon	238 ± 3	Xu et al. (2008)
20BS-116	Basalt	$^{206}Pb/^{238}U$	Zircon	260 ± 5	Fan et al. (2008)
SCHL-66	Ultramafic dyke	$^{206}Pb/^{238}U$	Zircon	262 ± 3	Guo et al. (2004)
TH-1	Gabbro	$^{206}Pb/^{238}U$	Zircon	263 ± 4	Shellnutt et al. (2011b)
Mianhuadi	Metagabbro	$^{206}Pb/^{238}U$	Zircon	259.6 ± 0.8	Zhou et al. (2013)
CD-0401	Granite	$^{206}Pb/^{238}U$	Zircon	261 ± 4	Zhong et al. (2007)
HGF-01	Gabbro	$^{206}Pb/^{238}U$	Zircon	259.3 ± 1.3	Zhong and Zhu (2006)
DS-01	Gabbro	$^{206}Pb/^{238}U$	Zircon	260 ± 0.8	Zhong and Zhu (2006)
PZH72	Leucogabbro	$^{206}Pb/^{238}U$	Zircon	263 ± 3	Zhou et al. (2005)
ZJ-3	Sediments	$^{206}Pb/^{238}U$	Zircon	257 ± 3	He et al. (2007)
SW-5	Sediments	$^{206}Pb/^{238}U$	Zircon	260 ± 5	He et al. (2007)
Xinjie	Gabbro	$^{206}Pb/^{238}U$	Zircon	259 ± 3	Zhou et al. (2002)
FL14	Diorite	$^{206}Pb/^{238}U$	Zircon	258 ± 3	Zhou et al. (2006)
FL7	Diabase	$^{206}Pb/^{238}U$	Zircon	260 ± 3	Zhou et al. (2006)
LM18	Gabbro	$^{206}Pb/^{238}U$	Zircon	263 ± 3	Zhou et al. (2008)
Zb4	Diorite	$^{206}Pb/^{238}U$	Zircon	261 ± 1	Zhou et al. (2008)
MY6	Syenite	$^{206}Pb/^{238}U$	Zircon	262 ± 2	Zhou et al. (2008)
20BS-71	Basalt	$^{40}Ar/^{30}Ar$	Whole rock	253.6 ± 0.4	Fan et al. (2004)
20BS-99	Basalt	$^{40}Ar/^{30}Ar$	Whole rock	255.4 ± 0.4	Fan et al. (2004)
20BS-119	Basalt	$^{40}Ar/^{30}Ar$	Whole rock	256.2 ± 0.8	Fan et al. (2004)
20BS-76	Basalt	$^{206}Pb/^{238}U$	Zircon	253.7 ± 6.1	Fan et al. (2004)
EM-90	Basalt	$^{40}Ar/^{30}Ar$	Whole rock	251.5 ± 0.9	Lo et al. (2002)
EM-PZH01	Syenite	$^{40}Ar/^{30}Ar$	Biotite	254.6 ± 1.3	Lo et al. (2002)
EM-37	Basalt	$^{40}Ar/^{30}Ar$	Whole rock	252 ± 1.3	Lo et al. (2002)
EM-MMG05	Syenite	$^{40}Ar/^{30}Ar$	Biotite	252 ± 1.3	Lo et al. (2002)
EM-PZH11	Syenite	$^{40}Ar/^{30}Ar$	Biotite	251.6 ± 1.6	Lo et al. (2002)
EM-86	Trachyte	$^{40}Ar/^{30}Ar$	Hornblende	252.8 ± 1.3	Lo et al. (2002)
EM-15	Basalt	$^{40}Ar/^{30}Ar$	Whole rock	255.9 ± 5.7	Lo et al. (2002)
Guanxi	Basalt	$^{206}Pb/^{238}U$	Zircon	257 ± 7	Lai et al. (2012)
Ch-97-90	Pyroxeneite	$^{40}Ar/^{30}Ar$	Phlogopite	254 ± 5	Boven et al. (2002)
Jinbaoshan	Wehrlite	$^{206}Pb/^{238}U$	Zircon	260.6 ± 3.5	Tao et al. (2009)
Jinbaoshan	Hornblendite	$^{206}Pb/^{238}U$	Zircon	260.7 ± 5.6	Tao et al. (2009)
CD-0701	Mafic enclave	$^{206}Pb/^{238}U$	Zircon	259.5 ± 2.7	Zhong et al. (2011)
CD-0703	Mafic enclave	$^{206}Pb/^{238}U$	Zircon	259 ± 3.1	Zhong et al. (2011)
BM-0703	Gabbro	$^{206}Pb/^{238}U$	Zircon	258.2 ± 2.2	Zhong et al. (2011)
TJ-0602	Syenite	$^{206}Pb/^{238}U$	Zircon	258.5 ± 2.3	Zhong et al. (2011)
TJ-0401	Syenite	$^{206}Pb/^{238}U$	Zircon	257.8 ± 2.6	Zhong et al. (2011)
CD-0401	Granite	$^{206}Pb/^{238}U$	Zircon	256.2 ± 1.5	Zhong et al. (2011)
WB-0703-1	Gabbro	$^{206}Pb/^{238}U$	Zircon	257.9 ± 2.4	Zhong et al. (2011)
WB-0703-1	Gabbro	$^{206}Pb/^{238}U$	Zircon	255.4 ± 3.1	Zhong et al. (2011))
WB-0701-1	Syenodiorite	$^{206}Pb/^{238}U$	Zircon	259.4 ± 1.1	Zhong et al. (2011)
WB-0701-6	Syenodiroite	$^{206}Pb/^{238}U$	Zircon	259.2 ± 1.3	Zhong et al. (2011)
20BS-76	Basalt	$^{206}Pb/^{238}U$	Zircon	259 ± 4	Fan et al. (2008)
WB-702	Syenodiorite	$^{206}Pb/^{238}U$	Zircon	257.8 ± 2.3	Zhong et al. (2011)
WB-705	Syenodiroite	$^{206}Pb/^{238}U$	Zircon	259.8 ± 1.6	Zhong et al. (2011)
WB-0604	Syenite	$^{206}Pb/^{238}U$	Zircon	255.8 ± 1.8	Zhong et al. (2011)
HG-0701	Gabbro	$^{206}Pb/^{238}U$	Zircon	258.7 ± 2	Zhong et al. (2011)
HG-0703	Gabbro	$^{206}Pb/^{238}U$	Zircon	258.9 ± 2.1	Zhong et al. (2011)
ALH-0401	Granite	$^{206}Pb/^{238}U$	Zircon	256.8 ± 2.8	Zhong et al. (2011)
ALH-0702	Granite	$^{206}Pb/^{238}U$	Zircon	256.2 ± 3	Zhong et al. (2011)
TH-0701	Gabbro	$^{206}Pb/^{238}U$	Zircon	258.8 ± 2.3	Zhong et al. (2011)
GS03-111	Mafic dyke	$^{206}Pb/^{238}U$	Zircon	257.6 ± 0.5	Shellnutt et al. (2012a)
GS05-005	Mafic dyke	$^{206}Pb/^{238}U$	Zircon	259.2 ± 0.4	Shellnutt et al. (2012a)
GS03-105	Mafic dyke	$^{206}Pb/^{238}U$	Zircon	259.5 ± 0.8	Shellnutt et al. (2012a)
GS05-067	Syenite	$^{206}Pb/^{238}U$	Zircon	259.6 ± 0.5	Shellnutt et al. (2012a)
DHS-1	Syenite	$^{206}Pb/^{238}U$	Zircon	259.1 ± 0.5	Shellnutt et al. (2012a)
GS05-059	Syenite	$^{206}Pb/^{238}U$	Zircon	258.9 ± 0.7	Shellnutt et al. (2012a)
GS04-143	Granite	$^{206}Pb/^{238}U$	Zircon	258.4 ± 0.6	Shellnutt et al. (2012a)
JW-1	Ignimbrite	$^{206}Pb/^{238}U$	Zircon	263 ± 4	He et al. (2007)
CT-2	Clayey tuff	$^{206}Pb/^{238}U$	Zircon	260 ± 4	He et al. (2007)

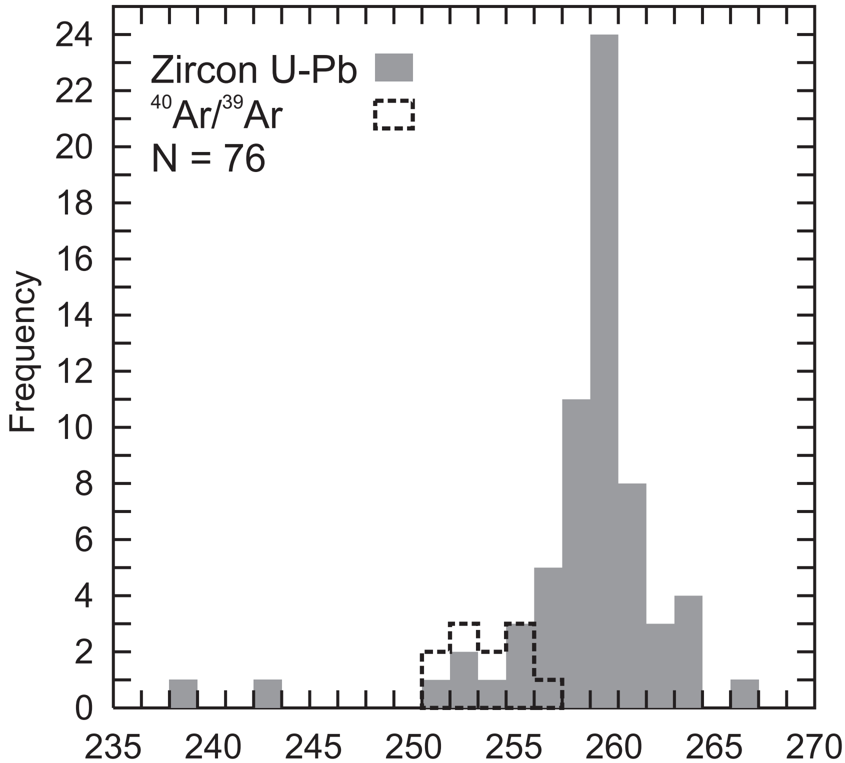

Figure 3. Frequency distribution of whole rock $^{40}Ar/^{39}Ar$ and zircon U/Pb radioisotopic age dates of rocks from the ELIP.

the precision, the estimates are at least 150 °C above the T_p estimates of primitive MORB values and thus indicative of a high temperature regime (Herzberg et al., 2007; Ali et al., 2010).

The ELIP picritic rocks can be subdivided into LREE-enriched, LREE-depleted and may be further subdivided into high-Ti (TiO_2 = 1.1–2.4 wt.%) and low-Ti (TiO_2 = 0.6–1.6 wt.%) varieties (Hanski et al., 2004, 2010; Zhang et al., 2006a, b; Wang et al., 2007; He et al., 2010c; Li et al., 2012). Li et al. (2010) however suggested that the picrites at Muli are better divided into three groups (i.e. Type-1, Type-2A and Type-2B) on the basis of γ_{Os} and $\varepsilon_{Nd}(t)$ and to a lesser extent HFSE data. Type-1 picrites are characterized as having $\gamma_{Os} = +7.5$ to $+11.5$ and $\varepsilon_{Nd}(t) = +6$ to $+8$ whereas the Type-2 picrites have $\gamma_{Os} = -4.2$ to -0.3 and $\varepsilon_{Nd}(t) < +6.5$. The γ_{Os} (i.e. $\gamma_{Os} = -2.4$ to -0.9) values reported by Zhang et al. (2008a, b) from Lijiang area are more similar to the Type-2 Muli picrites of Li et al. (2010). The Pb isotope data (i.e. $^{206}Pb/^{204}Pb$ = 17.933–18.883; $^{207}Pb/^{204}Pb$ = 15.513–15.589; $^{208}Pb/^{204}Pb$ = 37.93–38.85) of the picritic rocks were reported by Zhang et al. (2006a, b) indicate that they are similar to oceanic hotspots (i.e. Indian Ocean) and the Siberian Traps.

The formation of the ultramafic lavas is a ‘hotly’ debated topic. Similar to the ELIP as a whole, the basic facts are accepted but the details are contested. For example, there is general agreement that the ultramafic rocks erupted relatively early, they are primitive, high temperature melts and that they represent a large (i.e. >20%) amount of melting from a garnet-bearing mantle source (Hanski et al., 2004, 2010; Zhang et al., 2005, 2006a, b; Wang et al., 2007; Kamenetsky et al., 2012). However there are different interpretations regarding the nature and origin of the source. Kamenetsky et al. (2012) have suggested that the two series (i.e. high-Ti and low-Ti) of picrites are derived from separate mantle sources, a peridotite source for the low-Ti series and a garnet pyroxenite for the high-Ti series, and originate from the subcontinental lithospheric mantle which may be comprised of variable proportions of eclogite, garnet pyroxenite and peridotite rather than a deep-seated mantle plume source or asthenospheric source. In contrast, the prevailing view is that the ultramafic rocks are pristine primitive melts from the starting plume head that are in some cases, modified via interactions with one of or a combination of crustal material and lithospheric mantle melts and AFC processes (Hanski et al., 2004, 2010; Zhang et al., 2006a, b, 2008a, b; Wang et al., 2007; He et al., 2010c; Li et al., 2010). Wang et al. (2007) suggested that the differences in the Ti- and LREE-varieties are explained by higher degrees of anhydrous melting at shallow mantle depths (i.e. LREE-depleted) and the mantle source modified by subducted oceanic crust (i.e. LREE-enriched). Some of the picrites, although certainly not all, show the most depleted Sr-Nd-Os isotope signatures (i.e. $I_{Sr} \approx 0.7040$; $\varepsilon_{Nd}(t) \approx +8$; $\gamma_{Os} \approx +11$) in the entire ELIP and implies there is a depleted mantle (i.e. sub-lithosphere) component in some of the rocks (Hanski et al., 2004; Li et al., 2010, 2012). Therefore it is possible that some picrites represent original depleted mantle material which was modified by interactions with crustal material and possibly an SCLM component whereas other picrites are derived from an SCLM source.

4.2. The Emeishan flood basalts

The flood basalts are the signature feature of the ELIP and testify to a widespread mantle melting event. The total maximum thickness of basaltic flows is ~5 km located in the western portion (i.e. Yunnan) of the ELIP whereas in the eastern portion (i.e. Guizhou) total flow thickness is only a few hundred metres (Lin, 1985; Huang, 1986; Xu et al., 2001). The average flood basalt thickness throughout the entire region is estimated to be ~700 m (Lin, 1985).

The known area of the ELIP is considered to cover $\sim 0.25 \times 10^6$ km^2 with a total volume of $\sim 0.3 \times 10^6$ km^3 however there are suggestions that the volume was closer $\sim 0.6 \times 10^6$ km^3 and that the calculated total amount of material added to the crust was $\sim 8.9 \times 10^6$ km^3 (Lin, 1985; Wignall, 2001; Zhu et al., 2003). The original area and volume of the ELIP can only be speculated because the region has experienced substantial deformation associated with the amalgamation of the North China, South China and Indochina blocks during the early to middle Mesozoic and the early Paleogene Indo-Eurasian collision. Many mafic LIPs, such as the Siberian Traps or Central Atlantic Magmatic Province (CAMP), cover an area $>1 \times 10^6$ km^2 which dwarf the relatively modest size of the ELIP. This is not to say the ELIP is insignificant but rather that size is not a prerequisite in order to be geologically significant.

The early themes of Emeishan basalt studies was that they appeared to be readily divisible into two main compositional groups, with further sub-groupings (i.e. LT1, LT2, HT1, HT2 and HT3), on the basis of their TiO_2 wt.% and Ti/Y ratio and that there is a spatial-temporal distribution (Song et al., 2001; Xu et al., 2001, 2004; Xiao et al., 2004; He et al., 2010c; Zheng et al., 2010; Lai et al., 2012). The division into 'high-Ti' and 'low-Ti' groups corresponded to a petrological distinction as the 'high-Ti' (i.e. TiO_2 >2.5 wt.%) basalts were considered to be derived by low degrees (<8%) of partial melting of the pristine source whereas the 'low-Ti' basalts (i.e. TiO_2 < 2.5 wt.%) were considered to be derived from either the subcontinental lithospheric mantle (SCLM) or picritic magmas that assimilated upper crust (Xiao et al., 2004; Wang et al., 2007; Fan et al., 2008; Song et al., 2008; Zhou et al., 2008; He et al., 2010). The inference is that the type of basalt is indicative of the type of mineral deposit (i.e. sulphide or oxide) which may be present in the immediate area (Song et al., 2008a, 2009; Zhou et al., 2008; Wang et al., 2011). On the other hand, Xu et al. (2007) argued, based on Os, Pb and Nd isotope data, the opposite with the 'high-Ti' basalts are derived from the SCLM whereas the 'low-Ti' basalts are derived from the mantle plume source. The Ti-classification scheme, including the various sub-groupings, and hence the petrological connotation does not appear to be as robust as initially indicated (Hao et al., 2004; Hou et al., 2011; Shellnutt and Jahn, 2011). The Ti-classification scheme is somewhat arbitrary and that there is, in fact, a continuous spectrum of compositions rather than two distinct groups (Fig. 4).

The geographic distribution of the Emeishan basalts between the inner and outer zones has led to speculation that there is a consistent spatial, temporal and chemical relationship where the 'higher-Ti' basalts are located mostly in the outer zone and the 'lower-Ti' basalts are located mostly in the inner zone (Xu et al., 2001, 2004). The implication is that the 'higher-Ti' basalts represent the last eruptive rocks however the spatial-compositional variation is debatable and may not exist. It is known that some 'high-Ti' basalts are present within the inner zone however they were considered to be young as the 'low-Ti' basalts are typically the basal flows in this area. Although there are many stratigraphic profiles with basal 'low-Ti' basaltic flows (e.g. Binchuan, Ta Khoa, Chieng Ngam, Yangliuping, Ertan) there are almost an equal amount of sections which have basal 'high-Ti' flows, for example, Heishitou, Panzhihua, Longzhoushan, Yanyuan Suoi Chat and Doi Bu (Xu et al., 2001, 2003; Song et al., 2006; Qi and Zhou, 2008; Qi et al., 2008; Zheng et al., 2010; Anh et al., 2011; Shellnutt and Jahn, 2011). Additionally, 'high-Ti' mafic dykes have ages between 257 Ma and 260 Ma indicating that they are no more or less likely to be older or younger than other intrusive rocks in the inner zone (Shellnutt et al., 2012a). The concentration of the Fe-Ti oxide within the inner zone is also at odds with the spatial-compositional distribution because they are considered to have 'high-Ti' basaltic parental magmas and paleomagnetic data suggest that there is no definitive temporal relationship between the eruption of the 'low- and high-' Ti basalts (Zhou et al., 2008; Pang et al., 2009, 2010, 2013; Zheng et al., 2010; Shellnutt and Jahn, 2011). If there is a temporal-spatial-compositional relationship of the Emeishan basalts then more definitive evidence is required.

The Emeishan basalts are chemically similar to many continental tholeiities however the 'higher-Ti' basalts are more similar to OIB than the 'lower-Ti' basalts (Fig. 5). The whole rock Sr and Nd isotopes of the Emeishan basalts indicate that they could be derived from a heterogeneous mantle source, for example mixing between two distinct isotopic sources, and/or experienced variable degrees of crustal assimilation (Fig. 6). The typical range of the $\varepsilon_{Nd}(t)$ values of the Emeishan basalts is between −5 and +6 as both the 'high-Ti' basalts (i.e. $\varepsilon_{Nd}(t) = -3.6$ to $+4.8$) and the 'low-Ti' basalts (i.e. $\varepsilon_{Nd}(t) = -14.2$ to $+6.4$) completely overlap. Assuming the pristine end-member source of the Emeishan basalts has an $\varepsilon_{Nd}(t)$ value of +7, then more than 20% assimilation of Yangtze Block upper crustal rocks is required to reproduce the isotope trend observed in Fig. 6a. So much crustal assimilation is unlikely to occur because the rocks would no longer be basaltic in composition and assimilation would induce crystallization in the host magma before more assimilation could occur (Glazner, 2007). Furthermore, many Emeishan basalts that have low $\varepsilon_{Nd}(t)$ values (i.e. $\varepsilon_{Nd}(t) \geq 0$) also have trace element ratios, such as Th/Nb_{PM}, Nb/La, Ta/Yb that do not indicate so much crustal contamination is needed (Fig. 7). In other words, crustal contamination is not an end-member component in the Emeishan source material and that it likely occurs in varying proportions according to the precise emplacement conditions (e.g. location, country rock, amount of source melting, temperature). The major implication is that the Emeishan source is likely to be heterogeneous. The $^{206}Pb/^{204}Pb_1$ (18.3–20.6) ratios, positive Δ8/4 (67.7–83.0) and Δ7/4 (0.96–11.0) appear to support a heterogeneous source because Fan et al. (2008) interpreted the data as evidence for HIMU- and EM1-components and thus mantle plume-lithosphere interactions (Fig. 6b–d).

The source of the basalts, as with the ultramafic rocks, is a highly debated issue. There are suggestions the basalts are derived either directly from the SCLM or from sub-lithospheric source or as derivative melts from the picritic rocks (Song et al., 2001, 2004, 2008a, b; Xu et al., 2001; Hanski et al., 2004; Xiao et al., 2004; Hou et al., 2006; Wang et al., 2007; Fan et al., 2008; Zhou et al., 2008; Wang et al., 2011). Isotope data and trace elements can usually distinguish between possible source contributions but in the case of the ELIP they are not particularly insightful. The total range of $\varepsilon_{Nd}(t)$ for all of the mafic and ultramafic rocks is −10 to +8. The large range of Nd-isotopes is the same with the Sr (I_{Sr} ≈0.7040–0.7132), Os (γ_{Os} ≈ −5 to +11) and Pb isotopes ($^{206}Pb/^{204}Pb_1$ ≈ 17.9–19.7). Even if samples are screened for contamination there is still a large range. Trace elements are no more or less useful as there is a continuous compositional range across all of the basalts (i.e. 'high- and low-Ti') and the chemical trends which could be interpreted as crustal assimilation could in fact represent mixing between a subducted sediment component (e.g. GLOSS) and the mantle source (Fig. 7a–c). Therefore crustal assimilation, fractional crystallization of picritic magmas, amount of source melting, heterogeneous mantle, SCLM and mantle plume source cannot be individually ruled out as mechanisms or sources which have contributed to the basalt genesis. In other words, there is no consensus on the formation of the basalts beyond the fact that they were derived either indirectly or directly form some part of the mantle at 260 Ma. In all likelihood both lithospheric and sub-ithospheric mantle sources were tapped and that crustal assimilation occurred in some instances.

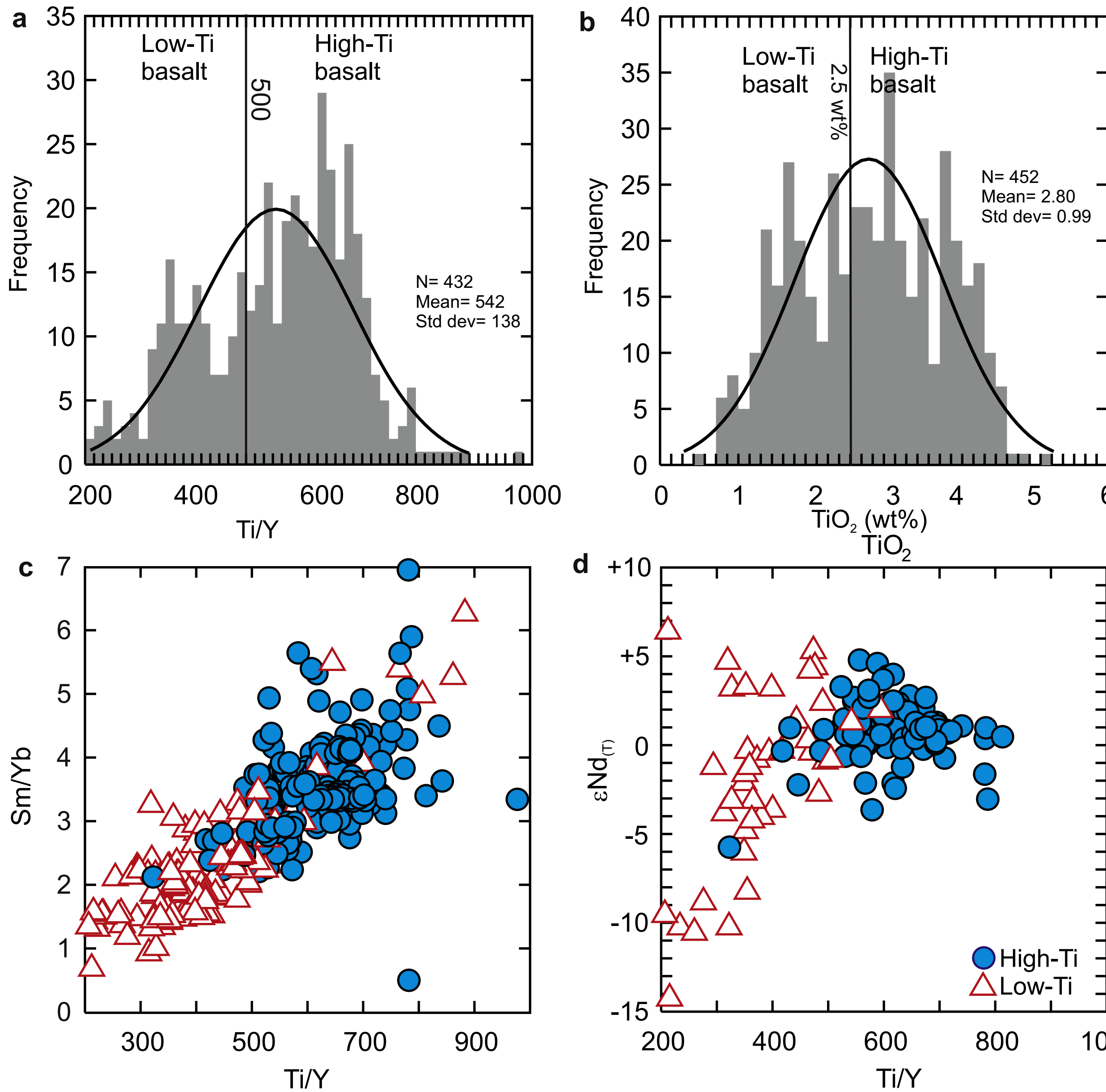

Figure 4. Frequency distribution plots of (a) Ti/Y showing the 500 division line and (b) TiO_2 (wt.%) showing the 2.5 wt.% division, (c) Sm/Yb ratio vs. Ti/Y of the Emeishan basalts showing a continuous trend and (d) the range of $\varepsilon_{Nd}(t)$ vs. Ti/Y. Data taken from Song et al. (2001, 2003, 2004, 2008a), Xu et al. (2001), Xiao et al. (2003, 2004), Hou et al. (2006), Wang et al. (2007), Fan et al. (2008), Qi et al. (2008), Qi and Zhou (2008), Shellnutt and Jahn (2011), Anh et al. (2011) and Lai et al. (2012).

4.3. Silicic rocks

The silicic volcanic and plutonic rocks of the ELIP are a volumetrically minor (i.e. $\leq$5%) component but testifies to the diversity of magmas that can be produced within large igneous provinces. In general, silicic volcanic rocks are commonly exposed in the upper portions of the flood basalt stratigraphy whereas the plutonic rocks typically remain buried with the rest of the magmatic pluming system. The ELIP is an excellent region to study the silicic rocks because both the volcanic and plutonic rocks are well exposed.

The silicic volcanic rocks of the ELIP are found within the upper third of the stratigraphy within the inner and Song Da zones. The silicic rocks classify as andesites, trachy-andesite, trachyte, rhyolite and ignimbrite and range in composition from peraluminous, metaluminous and peralkaline (Shellnutt and Jahn, 2010; Xu et al., 2010; Anh et al., 2011). The peralkaline rocks have positive $\varepsilon_{Nd}(t)$ values, Eu/Eu* < 1, LREE-enriched and have distinct negative primitive mantle normalized Ba, Sr and Ti anomalies. The geochemical data suggest that these rocks are derived by fractional crystallization of mafic magmas resembling the Ti-rich Emeishan basalt with minimal, if any, crustal assimilation (Shellnutt and Jahn, 2010; Xu et al., 2010). In contrast, the metaluminous to peraluminous rocks have $\varepsilon_{Nd}(t) \leq 0$, Eu/Eu* $\leq$ 1, LREE-enriched and have negative primitive mantle normalized Sr and Ti anomalies. Anh et al. (2011) have suggested that the metaluminous to peraluminous rocks represent extensive fractionation of higher-Ti Emeishan basaltic magma but, unlike the

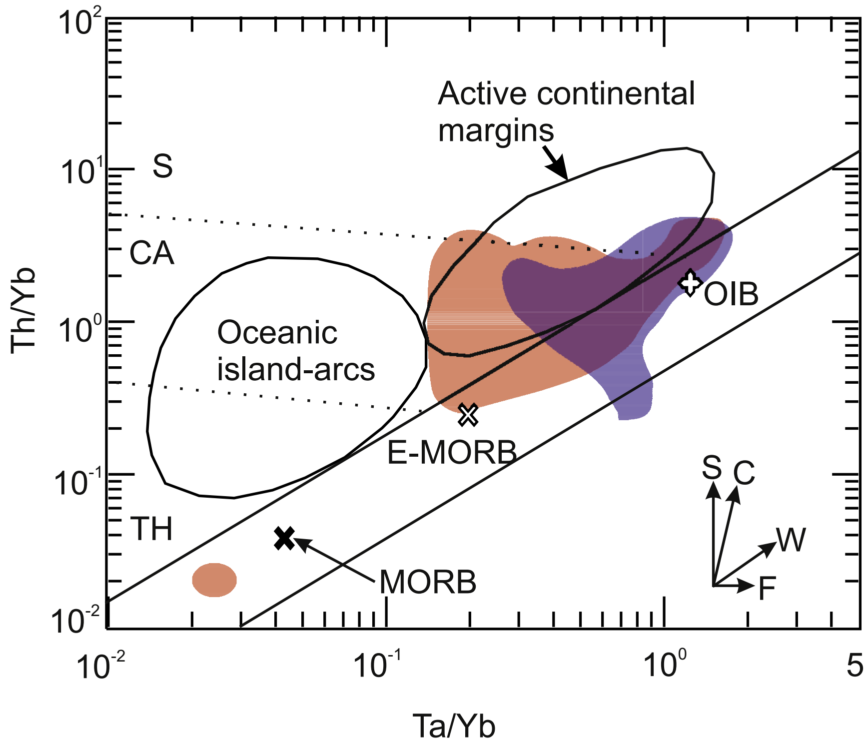

Figure 5. Th/Yb vs. Ta/Yb basalt tectonomagmatic discrimination diagrams of Wilson (1989) for the Emeishan basalts. S = shoshonitic, CA = calc-alkaline, TH = tholeiitic. The vectors are S = subduction component, C = crustal contamination, W = within-plate enrichment and F = fractional crystallization.

peralkaline rocks, assimilated crustal material. The stratigraphic position of the silicic rocks is consistent with a fractionation hypothesis because crust-derived melts should be closer to the lower portions of the volcanic pile (c.f. Shellnutt et al., 2012b).

The plutonic rocks of the ELIP range in composition from syenitic to granitic and, similar to the volcanic rocks, have alumina saturation indices (ASI) of peralkaline, metaluminous and peraluminous (Shellnutt and Zhou, 2007; Shellnutt et al., 2011b). The ASI values for the granitic rocks provide a relatively robust system for initial petrogenetic interpretations as the peralkaline rocks are considered to be derived by fractional crystallization of Emeishan mafic magmas, the metaluminous are either derived from mixing of mafic magmas and crustal material (i.e. hybrid) or by partial melting of underplated mafic rocks (i.e. mantle-derived) and the peralumuinous rocks are derived by crustal melting (Table 2) (Luo et al., 2007; Shellnutt and Zhou, 2007, 2008; Zhong et al., 2007, 2009, 2011a; Xu et al., 2008; Shellnutt et al., 2009a, b, 2011c, Shellnutt and Iizuka, 2012).

The peralkaline granitic rocks are defined by their chemical characteristics as having $Eu/Eu^* < 1.0$, $\varepsilon_{Nd}(t) > +1.5$; positive zircon $\varepsilon_{Hf}(t)$ values, negative Ba, Sr and Ti primitive mantle normalized anomalies and higher (i.e. >890 °C) temperature estimates (Shellnutt and Iizuka, 2011). The peralkaline rocks typically do not show much evidence for crustal assimilation although there is at least one pluton (i.e. Cida) where this may be the case (Zhong et al., 2007; Shellnutt et al., 2011c; Luo et al., 2013). The mantle-derived metaluminous granitoids are characterized by $Eu/Eu^* > 1.0$, $\varepsilon_{Nd}(t)$ values $\geq +1.5$; positive zircon $\varepsilon_{Hf}(t)$ values, depleted $Th\text{-}U_{PM}$ and $Zr\text{-}Hf_{PM}$ anomalies and positive Ba_{PM} anomalies and lower (i.e. <900 °C) temperature estimates whereas the hybrid metaluminous rocks do not have definitive chemical characteristics partially due to their mixed nature and the fact that few of these rocks have been identified but they have $Eu/Eu^* \approx 1.0$, $\varepsilon_{Nd}(t) = -0.7$ to $+1.4$ and zircon $\varepsilon_{Hf}(t) = +1.4$. The last group of granitic rocks are typically peraluminous but can be metaluminous and have characteristics such as $Eu/Eu^* < 1.0$, negative $\varepsilon_{Nd}(t)$ values, negative Nb-Ta primitive mantle normalized anomalies, and LREE enrichment with flat HREE chondrite normalized patterns. The peraluminous rocks are considered to be derived by crustal melting associated with the injection of high temperature Emeishan magmas (Shellnutt et al., 2011c). The zircon Hf isotopic data from the mantle-derived granitoids rocks have $\varepsilon_{Hf}(t) \approx +9$ which are higher than crustal-derived Emeishan granites but lower than depleted mantle (Xu et al., 2008; Shellnutt et al., 2009b). Furthermore the mantle-derived granitoids do not show compelling evidence (e.g. trace element ratios) for crustal assimilation and the $\varepsilon_{Hf}(t)$ values may be representative of their mafic parental source (Shellnutt et al., 2009b).

The formation of the silicic plutonic and volcanic rocks, in contrast to the basalts, is simpler in many respects. Simply put, the silicic rocks are either derived directly or indirectly (e.g. partial melting or fractional crystallization) from mafic magmas/rocks, by crustal melting or mixing of mafic magmas and crustal material. The petrogenesis of the silicic rocks can be more easily constrained than the basalts using Sr-Nd-Pb-Hf isotopes and trace element ratios.

5. Structural features and ecological impact of the Emeishan large igneous province

5.1. High velocity layers in the crust

Perhaps one of the most intriguing evidence in support of a mantle plume model for the ELIP is the differential high seismic layers within the Yangtze Block beneath the region considered to be the epicenter of magmatism (i.e. inner zone). The same region is shown to have thicker average crust than the middle and outer zones (Xu et al., 2004; Xu and He, 2007; Chen et al., 2010). The interpretation is that the deep high seismic velocity layers

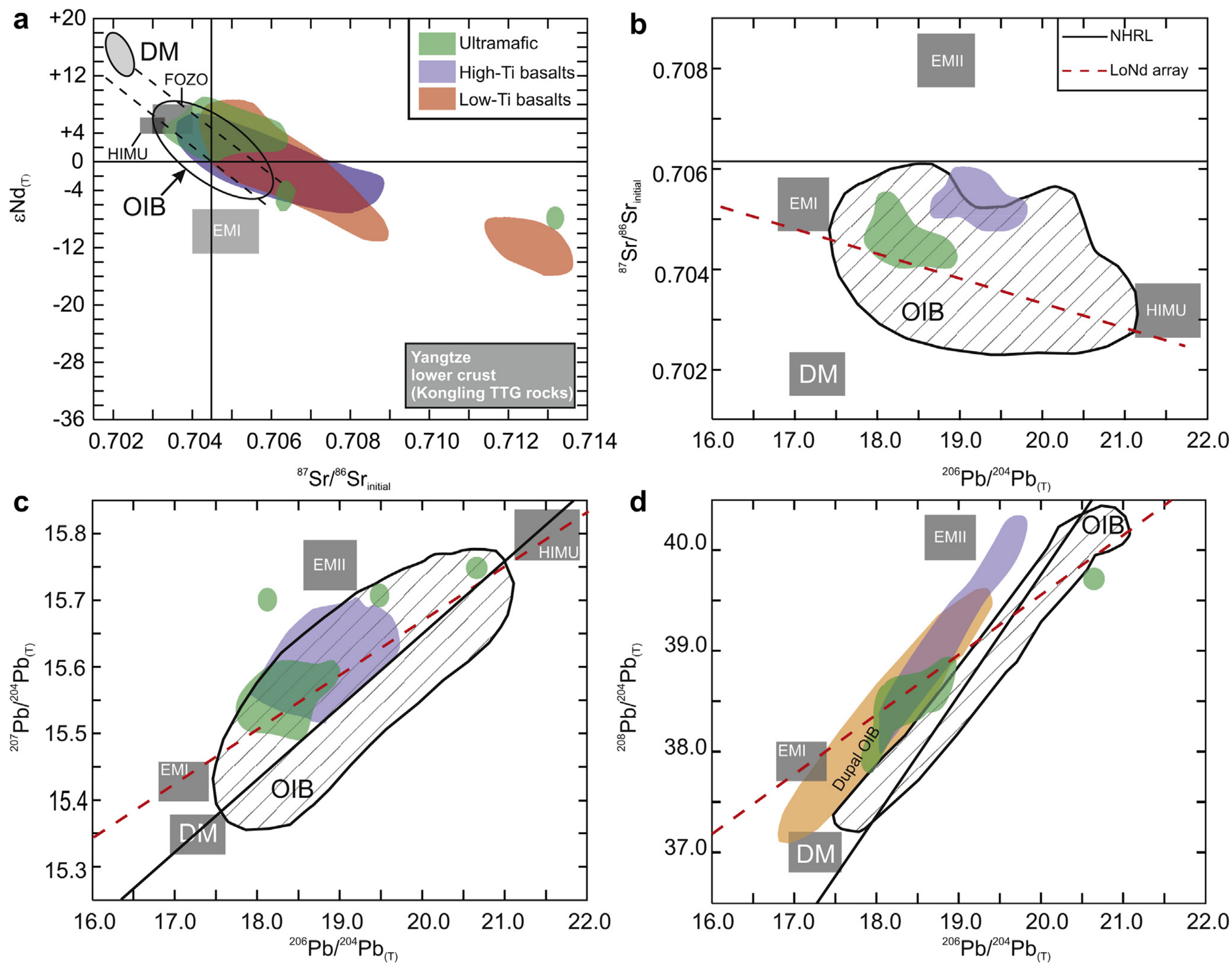

Figure 6. (a) Sr-Nd plot showing the known range of Emeishan ultramafic and mafic volcanic rocks. (b) $^{87}Sr/^{86}Sr_{initial}$ vs. $^{206}Pb/^{204}Pb_{(T)}$ plot of the Emeishan basalts from Guangxi and ultramafic rocks from Lijiang (western ELIP). (c) $^{207}Pb/^{204}Pb_{(T)}$ vs. $^{206}Pb/^{204}Pb_{(T)}$ of the Emeishan basalts from Guangxi and ultramafic rocks from Lijiang (western ELIP). (d) $^{208}Pb/^{204}Pb_{(T)}$ vs. $^{206}Pb/^{204}Pb_{(T)}$ of the Emeishan basalts from Guangxi and ultramafic rocks from Lijiang (western ELIP). Emeishan ultramafic and mafic data taken from Xu et al. (2001), Xiao et al. (2003, 2004), Song et al. (2004, 2008a, b), Hou et al. (2006), Wang et al. (2007), Fan et al. (2008), Qi et al. (2008), Qi and Zhou (2008), Shellnutt and Jahn (2011), Anh et al. (2011), Kamenetsky et al. (2012) and Lai et al. (2012). EMI and HIMU range taken from Zindler and Hart (1986). GLOSS (global subducting sediment) values taken from Plank and Langmuir (1998) and Chauvel et al. (2008). FOZO range taken from Hart et al. (1992) and Campbell (2007). The range of Yangtze Block lower crust rock compositions taken from Wang et al. (2007).

represent the fossilized mantle plume head whereas the lower crust high velocity layers represent underplated mafic and ultramafic rocks from the plume head which fed the surface flows and shallow crustal intrusions (Fig. 2b). The seismic data interpretations coupled with the crustal thickness is a very elegant explanation for and is consistent with what would be expected from a mantle plume model however there is a possible alternative explanation (Campbell, 2007).

The crustal seismic layers cannot be completely attributed to the ELIP. For example, the seismic layers could represent a mixture of mafic and ultramafic material from an earlier magmatic event. The western margin of the Yangtze Block was the site of either long-lived subduction-related magmatism or mantle plume-related magmatism during the Neoproterozoic (Li et al., 1999; Zhou et al., 2002b; Zhao and Zhou, 2007). The reason for the magmatism is irrelevant, because, whatever the cause, there are significant amounts of mafic and felsic plutonic rocks along the entire western margin of the Yangtze Craton. Given that most of the Neoproterozoic felsic and mafic intrusive rocks found within ELIP inner zone have continental-arc affinity, it is very possible that magmas accumulated in the lower crust of the Yangtze Block during this time and served as a source or contaminant for the ELIP basalts (Zhao and Zhou, 2007). The Emeishan basalts have $\varepsilon_{Nd}(t)$ values ranging from −14.2 to +8.0 which encompasses both varieties of basalts and most of the ultramafic rocks. The T_{DM} model ages range between 640 and 2400 Ma. The large range in Nd isotope composition is explained, in most cases, as either evidence for crustal contamination or an isotopically heterogeneous source. If the samples with minimal or no evidence for crustal assimilation (i.e. $Th/Nb_{PM} < 3$ and $\varepsilon_{Nd}(t) < +2$), are considered then the T_{DM} model ages have a more restricted range (i.e. 640 Ma to 1400 Ma) which partially overlaps with the age of the Neoproterozoic rocks. The T_{DM} values suggest that the Emeishan source, in comparison to the emplacement age, is an ancient reservoir. The T_{DM} ages could support a mantle plume model in the sense that the mantle material is coming from a deep source that was last modified around 900 Ma or it could mean a source which was mixed with an ancient (subduction?) component at ∼900 Ma.

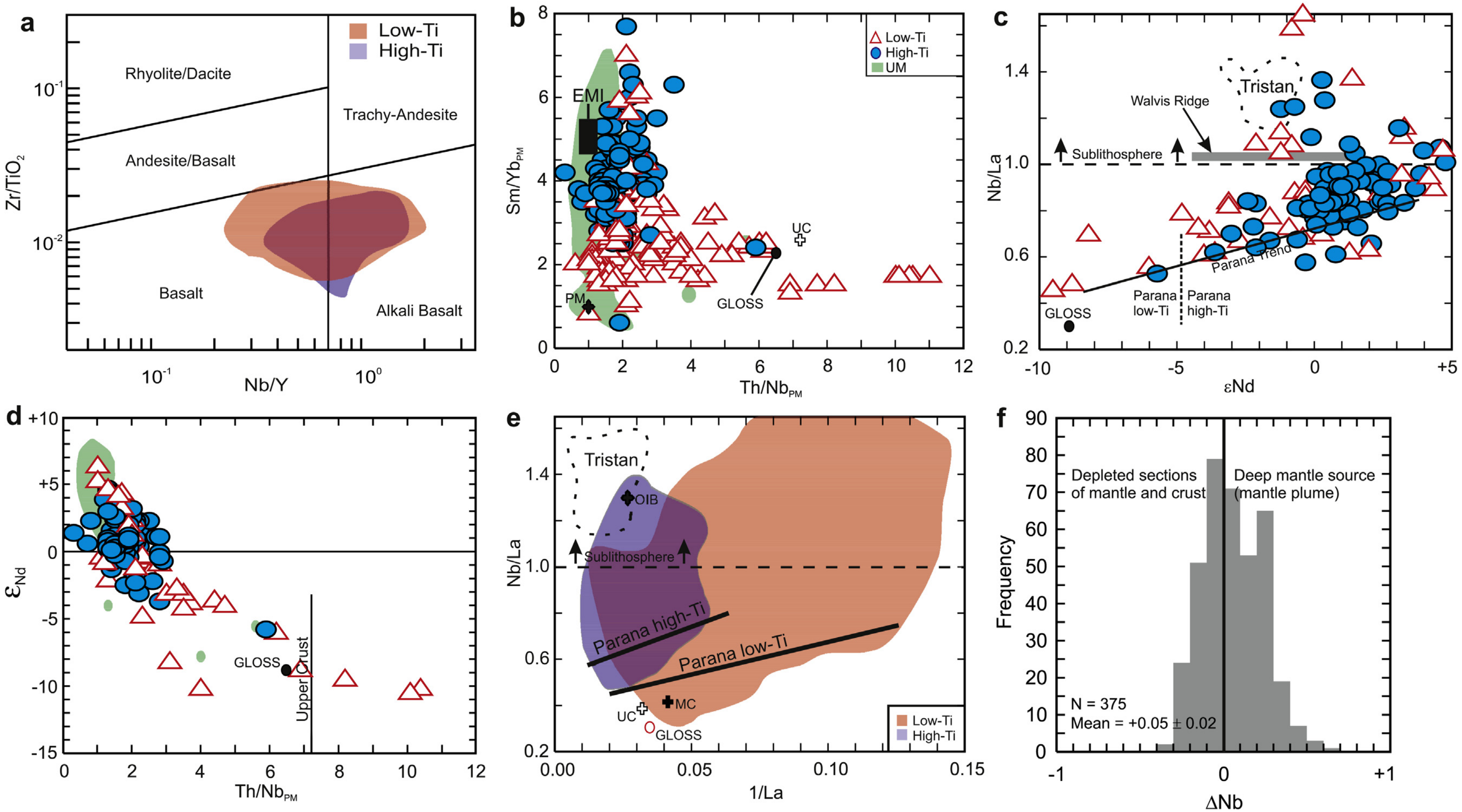

Figure 7. (a) Comparison of the Emeishan basalts using the discriminating parameters of Winchester and Floyd (1977). (b) Sm/Yb_{PM} vs. Th/Nb_{PM} of the basaltic rocks of the ELIP. (c) Nb/La vs. ε_{Nd} of the Emeishan basalts showing the trend of the Parana basalts for comparison. (d) ε_{Nd} vs. Th/Nb_{PM} of the basaltic and picritic rocks of the ELIP. (e) Nb/La vs. 1/La of the 'high- and low-Ti' Emeishan and Parana basalts. The fields of Tristan da Cunha, Walvis Ridge and trend lines of the Parana basalts are from Hawkesworth and Scherstein (2007). (f) The range of ΔNb ($\Delta Nb = \log[Nb/Y] + 1.74 - 1.92\log[Zr/Y]$) values of the Emeishan basalts. Values <0 are attributed to depleted sections of the mantle and crust whereas values >0 are attributed to deep mantle sources (Fitton et al., 1997; Baksi, 2001). Emeishan ultramafic and mafic data taken from Xu et al. (2001), Xiao et al. (2003, 2004), Song et al. (2004, 2008a, b), Hou et al. (2006), Wang et al. (2007), Fan et al. (2008), Qi et al. (2008), Qi and Zhou (2008), Shellnutt and Jahn (2011), Anh et al. (2011), Kamenetsky et al. (2012) and Lai et al. (2012). PM = Primitive mantle normalized to values of Sun and McDonough (1989). OIB = average ocean island basalts from Sun and McDonough (1989). EMI range taken from Zindler and Hart (1986) and Cliff et al. (1991). GLOSS (global subducting sediment) values taken from Plank and Langmuir (1998) and Chauvel et al. (2008). UC = upper crust, MC = middle crust values of Rudnick and Gao (2003).

Table 2
Summary of chemical characteristics of ELIP silicic rocks.

Type	Genesis	ASI	Eu/Eu*	$\varepsilon_{Nd}(t)$	$\varepsilon_{Hf}(t)$	T_{Zr} (°C)	Ba_{PM}	Nb-Ta_{PM}	Examples
Mantle	Fractional crystallization	Weakly peralkaline	<1.0	+1.5 to+3.4	+8.7 ± 0.4 to +9.2 ± 1.0	860 ± 17 897 ± 14 940 ± 21 953 ± 62	−ve	None	Baima, Taihe, Panzhihua (Dianchang), Cida?
	Partial Melting	Metaluminous	>1.0	+1.3 to+3.2	+5.8 ± 0.3 to +8.6 ± 0.2	723 ± 18	+ve	None	Woshui, Huangcao and Daheishan
Crust	Crust	Peraluminous to Metaluminous	<1.0	−6.7 to −3.9	−2.6 ± 0.4	767 ± 14	+ve or −ve	−ve	Ailanghe, Yingpanliangzi
Hybrid	Crust + Mantle	Metaluminous	≈1.0	−0.7 to +1.4	+1.4 ± 0.9		+ve	None	Maomaogou, Salian

Data is complied from Luo et al. (2007), Shellnutt and Zhou (2007, 2008), Zhong et al. (2007, 2009), Xu et al. (2008), Shellnutt et al. (2009a, b, 2011c). ASI is the alumina saturation index (Al/Ca−1.67P + Na + K); Eu/Eu* = [2*Eu_N/(Sm_N + Gd_N)] normalized to C1 chondrites of Sun and McDonough (1989); T_{Zr} is the zircon saturation thermometry; Ba_{PM} and Nb-Ta_{PM} indicate the presence of anomalous primitive mantle normalized values.

It is likely that the high velocity seismic layers represent the fossilized remnants of the Emeishan magmas however there is no age constraints on these layers. Therefore the high velocity layers could represent pure Emeishan material, pure Neoproterozoic material or an accumulation of both and there remains a possibility that the underplated Neoproterozoic rocks may have modified the original Emeishan magmas during their emplacement and is the reason why the basalts have higher-Ti concentration than most LIPs.

5.2. Flexure of the crust

It is theorized that the excessive heat (i.e. 100–350 °C above ambient conditions) from a mantle plume is suitable, depending on the exact thermal conditions, to induce maximum uplift of the surface directly beneath the plume head to an area within a 200 km radius. The amount of vertical displacement may be in excess of ~1 km (Griffiths and Campbell, 1991; Campbell, 2005). Flexure and doming of the crust prior to flood basalt eruption is considered to be one of the most compelling physical evidence for the presence of an ancient mantle plume (Cox, 1989; Campbell and Griffiths, 1990; Griffiths and Campbell, 1991; Rainbird, 1993; Farnetani and Richards, 1994; White and McKenzie, 1995; Campbell, 2005, 2007; Ernst et al., 2005; Saunders et al., 2005, 2007). It is also one of the most debated topics in LIP research as evidence for uplift and doming may not be as robost as purported nor necessary (Burov and Guillou-Frottier, 2005; Elkins and Tanton, 2007; Sheth, 2007b; Utskins-Peate and Bryan, 2008).

The ELIP is considered to be one of the best examples of mantle plume-induced surficial uplift and doming (Campbell, 2005, 2007). The progressive thickening of the Maokou limestone from the inner zone to the outer zone of the ELIP encapsulates the evidence for uplift and subsequent erosion and redisposition (Fig. 8a) (He et al., 2003, 2007; 2010a, b). However, the uplift model for the ELIP has come under scrutiny and alternative ideas have been presented (Utskins-Peate and Bryan, 2008, 2009; Ali et al., 2010; Sun et al., 2010; Utskins-Peate et al., 2011). The evidence against uplift is twofold: (1) that uplift either did not occur before volcanism or that pre-eruption uplift is muted (Ali et al., 2010; Sun et al., 2010) and (2) that the flood basalts were emplaced at sea-level and that previously interpreted alluvial fan sediments are actually hydromagmatic deposits (Utskins-Peate and Bryan, 2008, 2009; Utskins-Peate et al., 2011). The core of the debate is focused on whether the geological evidence presented by He et al. (2003, 2007, 2010a, b) is actually documenting uplift not whether the ELIP is or is not a mantle plume-derived LIP (Ali et al., 2010).

There is further geological evidence which argues against plume-induced uplift of the surface. The Panzhihua layered gabbro complex located in the Panxi region of the inner zone has intruded Sinian (~600 Ma) aged marbles whereas the granite portion, located stratigraphically above the gabbro of the complex intruded Emeishan flood basalts (Shellnutt and Jahn, 2010). The geological relationships indicate there is a conundrum. In order for the granite to intrude the basalts they must have erupted first. That means the basalts either erupted onto something which was overlying the Sinian limestones or directly on top of them. In either case the entire Paleozoic up to the Maokou limestones is missing (He et al., 2010a). Since the Panzhihua complex is intrusive, albeit shallow, the whereabouts of the Paleozoic rocks is unknown. The Paleozoic rocks could have been eroded before the deposition of the Maokou limestone or they were never deposited in the first place because they were above sea-level. If the Paleozoic rocks were eroded then why and how did conditions change so that the Maokou limestone could be deposited just before the Emeishan basalts erupted and why was the Paleozoic section preserved elsewhere (i.e. Dulong-Song Chay) on the Yangtze Block (Yan et al., 2006)? Perhaps the easiest explanation is that the Paleozoic rocks were not deposited because the inner zone was probably a topographic high (Fig. 8b), e.g. similar to the modern day Mascarene Plateau, and sea level may not have been sufficiently high to allow for deposition of carbonate rocks until the late Capitanian. The sea-level curve by Haq and Schutter (2008) show that the short-term sea-level change (Fig. 9) was the highest at the Capitanian–Wuchiapingian boundary which is contemporaneous with the eruption of Emeishan basalts onto the Maokou limestones (Gradstein et al., 2004; He et al., 2007, 2010a; Sun et al., 2010). If sea-level increased during the late Capitanian and the inner zone (i.e. Chuandian old land) was a topographic high then carbonate rocks would be deposited in sync with the increasing sea-level and thus given an appearance of a dome shape (Fig. 8b). If the 'topographic high' model is correct then it would also be consistent with thick crust beneath the inner zone of the ELIP because after uplift the dome would eventually erode away and presumable the Yangtze crust would become relatively thinner over time (Xu et al., 2004). Whatever the case may be, e.g. uplift or not, the argument against uplift is compelling and will require more evidence to refute but until such evidence is presented it will probably remain one of the most contentious debates in ELIP studies.

5.3. Effect on the late Permian ecosystem

There is a tendency to connect biological crises or mass extinctions with the eruption of subaerial or subaqueous flood basalts with contemporaneous or pene-contemporaneous volcanic (Rampino and Stothers, 1988; Courtillot et al., 1999; Wignall, 2001, 2005; White, 2002; White and Saunders, 2005). In many cases there is compelling evidence to link specific volcanic episodes to a

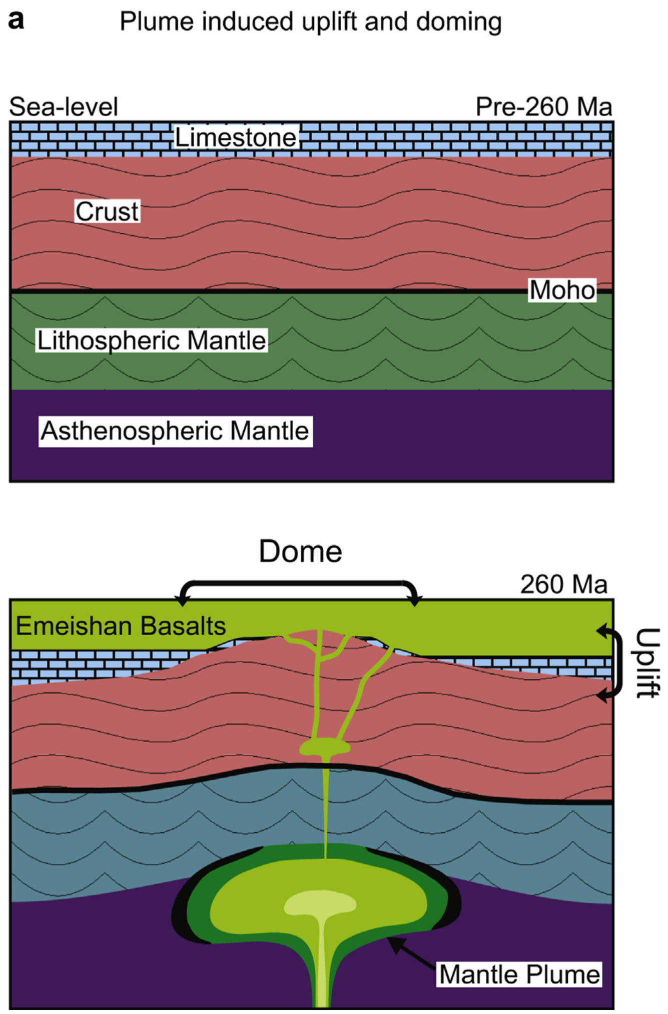

Figure 8. (a) Model of uplift and doming of the crust due to the arrival of the Emeishan mantle plume based on He et al. (2003, 2007, 2010a). (b) Alternatively the area around the western Yangtze Block was a topographic high and subsequent sea-level change allowed for deposition of carbonate rocks prior to the arrival of the Emeishan mantle plume.

decline in biota however there are many large igneous provinces (e.g. Tarim, Panjal, Karoo, Ethiopia, Columbia River) in which there is no association with ecosystem collapse. The basic premise is that, due to rapidly emplaced basaltic magmas, dramatic climatic changes occur at a pace which is faster than then ability of an ecosystem to adapt (Rampino and Stothers, 1988; Wignall, 2001). Whether the volcanism is responsible for a 'nuclear winter' scenario, exacerbates 'greenhouse' conditions or changes marine water chemistry is debated (Wignall, 2001; Saunders, 2005; Self et al., 2005). Some of the most severe mass extinctions such as the end-Permian, Cretaceous–Tertiary and Triassic–Jurassic are contemporaneous with major flood basalt eruptions.

Compared to the end-Permian mass extinction the late Capitanian mass extinction (~263 Ma) affected less genera but it was contemporaneous with the earliest eruption of the Emeishan flood basalts and as a consequence is considered to have been the cause of or at least contributed to the decline in biota at that time (Wignall, 2001; Zhou et al., 2002a; He et al., 2007; Ganino et al., 2008; Retallack and Jahren, 2008; Ganino and Arndt, 2009; Shellnutt et al., 2012a). If the atmosphere is to be affected by magmatism then emplacement rates have to be considerably fast. It is suggested that the emplacement of ELIP magmas into carbonate-rich country rocks and a rapid emplacement (i.e. <2 Ma) was sufficient to contribute significant enough amounts of CH_4 and thus induce a climate change or affect marine chemistry to the point where some genera would be vulnerable and die out (Ganino and Arndt, 2009; Shellnutt et al., 2012a).

It is possible that the ELIP either directly caused or accelerated the late Capitanian mass extinction however there are larger eruptions of flood basalts which clearly had no effect on global ecosystems (e.g. Tarim). The reason why some LIPs are contemporaneous with mass extinctions could be related to random conditions which cannot easily be predicted such as: parental magma composition, geographic location, composition of country rock, or vulnerability of species. The fact that continental flood basalts erupt on average of once per 20 Ma then the frequency of mass extinctions will undoubtedly match, at some point, with the formation of an LIP. So it seems that the ELIP may have erupted at the right time, in the right place and within the right country rocks (i.e. carbonate rocks).

6. Metalllogenesis of the Emeishan large igneous province

6.1. Ni-Cu sulphide and PGE deposits

The magmatic sulphide deposits are concentrated within ultramafic and/or mafic intrusive rocks and are found throughout the entire ELIP. The deposits contain variable proportions of Ni, Cu and

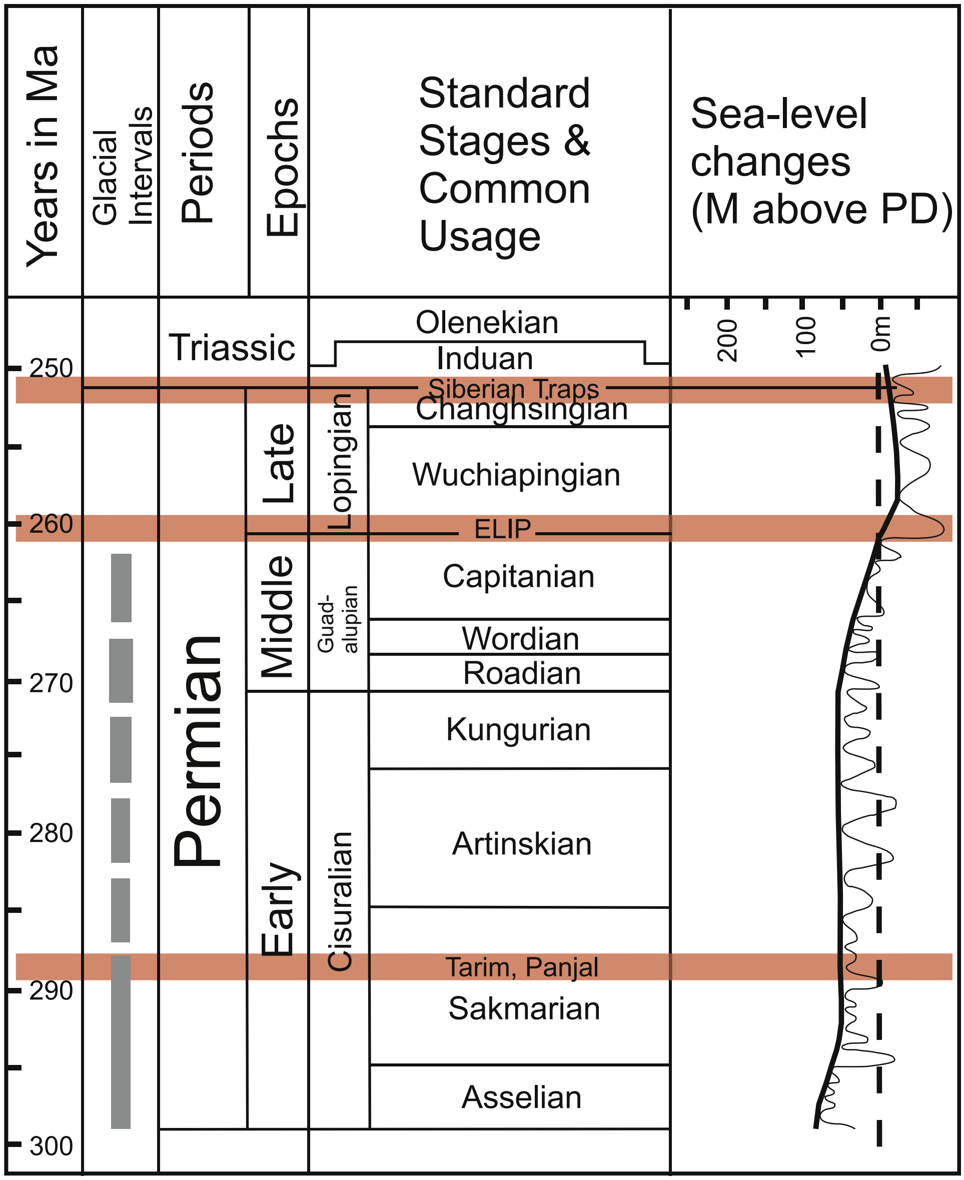

Figure 9. Sea-level changes, glacial intervals (grey rectangles) and eruption of continental flood basalts (red) during the of the Permian (modified from Haq and Schutter, 2008).

platinum group elements (PGE) within sulphide minerals or platinum group minerals (Zhong et al., 2002; Song et al., 2003, 2005, 2008a; Wang and Zhou, 2006; Wang et al., 2011). The propensity of sulphide and/or PGE deposit to form is suggested to be linked with the type (i.e. 'low-Ti') of parental magma (Song et al., 2003, 2008a, 2009; Zhou et al., 2008; Wang et al., 2011). Song et al. (2005) grouped the sulphide and PGE deposits into four genetic types based on petrogenetic processes and host rock and mineral associations. The four-types of deposits are (1) Ni-Cu-(PGE) by *in situ* sulphide segregation, (2) PGE-enriched layers within layered intrusions, (3) Ni-Cu sulphide related to sulphide-bearing mush and (4) PGE sulphide ores in ultramafic rocks. Native Cu and Au deposits have also been identified but the appear to be related to post-ELIP hydrothermal processes (Wang et al., 2006a, b; Zhang et al., 2006a, b; Zhu et al., 2007).

6.1.1. Ni-Cu-(PGE) sulphide deposits

The best example of this type of sulphide deposit is found in the Yangliuping area of Sichuan where numerous mafic-ultramafic sills (e.g. Yangliuping, Zhengziyanwuo, Xiezuoping, Daqiangyanwuo) have intruded mid to late Paleozoic metasedimentary rocks (Song et al., 2003). The sills range in size but are generally 2 km long and up to 300 m thick and composed of serpentinite (40–60%), talc schist (25–45%), tremolite schist (10–30%) and a minor amount of gabbro (5–7%) indicating substantial post-emplacement alteration and metamorphism occurred (Song et al., 2003). The sills (i.e. Yangliuping and Zhengziyanwuo) are estimated to contain 0.27 Mt of Ni, 0.10 Mt of Cu and 35 tons of PGE (Song et al., 2005). The ore bodies are found as either: (1) disseminated within the serpentinite, (2) massive ores within the footwall of the country rock (i.e. Paleozoic marble) or (3) mineralized veinlets within the intrusions (Song et al., 2003). The sills are considered to have formed from magmas which are compositionally similar to the basalt in the immediate area (Song et al., 2003, 2006). The general model is that basaltic magmas were emplaced and began to fractionate. The residual liquid becomes more evolved and at the same time volatiles (i.e. S, CO, CO_2) from the country rocks will be fluxing the magma system. The CO and CO_2 would decrease the magma oxidation state, and coupled with the decrease in magma temperature, crystallization and assimilation of S, promote S-oversaturation and sulphide immiscibility and the segregation and concentration of Ni, Cu and PGE within the sulphide liquid (Song et al., 2003). The sulphide liquid would concentrate at the bottom of the chamber and form the massive sulphide deposits whereas the disseminated and veinlet deposits represent sulphide liquid which was transported with the silicate magma during continued injection of new batches of magma and dispersed.

6.1.2. PGE-rich layers within layered intrusions

There are at least two mafic-ultramafic layered intrusions which host PGE-enriched layers. The Hongge and Xinjie intrusions are located in the central part of the Panxi region. The Hongge layered mafic-ultramafic intrusion contains PGE-rich layers in lower parts but is also the second largest Fe-Ti-V oxide deposit after Panzhihua. The Hongge intrusion is comprised of three main zones with four cycles which consist of variable proportions of olivine, clinopyroxene, magnetite, chromite and plagioclase with additional minor amounts of apatite, orthopyroxene and ilmenite (Zhong et al., 2002). The lower olivine zone (i.e. LOZ) is composed mostly of olivine, magnetite, clinopyroxene with hornblende and some plagioclase in the upper parts. The middle clinopyroxene zone (i.e. MCZ) begins with an olivine clinopyroxenite layer at the base and ends with a plagioclase clinonpyroxenite at the top. The upper gabbro zone in compositionally more evolved and contains more plagioclase. There are intermittent bands of magnetite starting from the lower MCZ and ending near the top of the UGZ. The LOZ does not contain an oxide-rich layer but lower part of the zone has a PGE-enriched layer and the boundary between the LOZ and MCZ is another PGE-enriched horizon. The LOZ is considered to be cycle I, the MCZ has cycles II and III and the UGZ is cycle IV. Each cycle is recognized by abrupt reversals in major and trace elemental values which indicate periods of crystallization and magma recharge suggesting Hongge was an open magma system (Zhong et al., 2002, 2003, 2005). The whole rock Sr-Nd isotopes (I_{Sr} = 0.7059–0.7072; $\varepsilon_{Nd}(t) = -2.7$ to $+1.0$) indicate that wall rock assimilation played a role in the segregation of sulphide-rich liquid and the formation of the PGE-rich layers but the repetitive formation of the oxide-rich layers are likely forming due to crystallization and magma recharge (Pang et al., 2008a; Bai et al., 2012a, b). The parental magma or magmas of the Hongge system is unknown but it was likely a mixture of more primitive mafic or ultramafic and basaltic magmas because the LOZ contains relatively minor amounts of plagioclase, bulk $Mg^{\#}$ increases abruptly at the cycle II–III boundary and the primitive mantle normalized PGE patterns of the magnetite-rich layers are similar to the ELIP picrites (Zhong et al., 2005; Bai et al., 2012a, b).

The Xinjie mafic-ultramafic layered intrusion is similar to the Hongge intrusion in terms of its isotope variability (e.g. I_{Sr} = 0.7056–0.7074; $\varepsilon_{Nd}(t) = -4.1$ to $+2.8$), cyclic ultramafic-mafic layered nature and presence of PGE-rich layers at the base followed by Fe-Ti oxide-rich layers in the middle to upper portion (Zhong et al., 2004, 2011b; Wang et al., 2008a; Zhu et al., 2010). The intrusion consists of three cyclic zones of ultramafic (i.e. wehrlite, clinopyroxenites) to mafic (i.e. gabbro) rocks which have variable proportions of clinopyroxene, olivine, plagioclase, oxide minerals (i.e. magnetite, ilmenite, ferrichromite, chromite), hornblende and sulphide minerals. The parental magma composition is unknown and whether it is mafic or ultramafic is debated (Zhong et al., 2004, 2011b; Wang et al., 2008a; Zhu et al., 2010). There are abrupt chemical and mineralogical changes between each cycle which is interpreted to represent injection of a new magma (Zhong et al., 2004, 2011b). The formation of the PGE deposits in the lower portions of the intrusion is thought to be due to wall rock assimilation-induced sulphide segregation but it is possible that the crystallization of magnetite may have caused subsequent S-saturation and allowed the PGE to partition into sulphide minerals (Zhu et al., 2010). The oxide-rich layers on the other hand are probably due to simple crystallization processes and magma recharge (Wang et al., 2008a).

6.1.3. Ni-Cu sulphide-bearing mush

The sulphide mush-type of deposit is considered to be the most important type of sulphide deposit in the ELIP (Song et al., 2005). The deposits are typified by the Limahe and Baimazhai intrusions which contain 0.1–3 Mt of Ni ore and composed of gabbros, wehrlites, olivine peridotites, pyroxenites and massive sulphide ores (Wang and Zhou, 2006; Wang et al., 2006a, b; Pu et al., 2007; Sun et al., 2008; Tao et al., 2008, 2010; Zhang et al., 2009). The basic premise for the sulphide mush-type of deposit is that a mafic or ultramafic silica saturated, Mg-rich and S-undersaturated magma assimilated country rock at depth in a staging chamber (Wang and Zhou, 2006; Wang et al., 2006a, b; Sun et al., 2008; Tao et al., 2008, 2010). The magma became S-saturated due to contamination ($\delta^{34}S = +2.4‰$ to $+5.4‰$; $\gamma_{Os}(t) = \leq +263$; $I_{Sr} > 0.7075$; $\varepsilon_{Nd}(t) < 0$) from the country rock and promoted crystallization of mafic silicate minerals and thus the sulphide-rich portion settled to the base of the chamber. The precise mechanism of sulphide transportation or concentration may be different between Limahe and Baimazhai but they represent dynamic magma systems. In the case of the Baimazhai deposit, the upper part of the chamber is silicate-rich and expelled whereas the lower portion is a mixture of silicate and sulphide and subsequently the entire system is squeezed allowing for the complete expulsion of the more evolved silicate magma and the zonation of the silicate and sulphide-rich mixture (Wang and Zhou, 2006; Wang et al., 2006a, b).

6.1.4. PGE sulphide ores within ultramafic rocks

The PGE sulphide ore deposit is mainly described from the Jinbaoshan ultramafic sill located east of Dali in Yunnan Province and is ~5 km long, 1 km wide and variably thick ranging between 20 and 150 m. The sill intrudes Devonian dolomite which overlies the Proterozoic basement rocks of the Yangtze Block. The stratigraphy of the intrusion is rather simple as it is composed of wehrlite with intermittent layers of disseminated sulphide Pt-Pd mineralization at quasi regular intervals whereas there is a 5–15 m layer of chromite in the middle of the intrusion. There are gabbros located in the upper portion of the intrusion but probably not petrogenetically related to the Jinbaoshan parental magmas and hornblende pyroxenite is occasionally found at the margins (Wang et al., 2005, 2008b, 2010; Tao et al., 2007, 2009). Nevertheless, Brozdowski et al. (2004) divided the Jinbaoshan intrusion into six units which are based on variations in mineralogy and textures (i.e. grain size, mode). The concentration of the Pt + Pd typically ranges from 1 ppm to 5 ppm with occurrences as high as 17 ppm whereas Ni and Cu have grading of ~0.21% and ~0.16% respectively. The total amount of Pt + Pd is ~45 tons (Tao et al., 2007; Wang et al., 2008b). The two main economic horizons are referred to as K_1 and K_2 and range in thickness from 4 m to 16 m. The K_1 horizon is located at the base of the intrusion whereas the K_2 is located at the base of the fifth horizon (Brozdowski et al., 2004). The Jinbaoshan intrusion is likely derived from a Mg-rich, Ti-poor tholeiitic parental magma and, according to Tao et al. (2007), represents a residual assemblage formed by the magmatic dissolution of plagioclase due to multiple pulses. Wang et al. (2005) suggested there is limited evidence (i.e. $\varepsilon_{Nd}(t) = -0.1$ to $+0.8$, $\gamma_{Os}(t) = +20.7$ to $+77.8$, $\delta^{34}S = 0.6$ to $2.8‰$) for crustal contamination. It is thought that sulphide saturation of the parental magma occurred at depth due to olivine and chromite crystallization and that the subsequent immiscible sulphide droplets were transported and accumulated in the Jinbaoshan sill through successful magma pulses (Tao et al., 2007; Wang et al., 2010). Hydrothermal fluids likely contributed to the formation or redistribution of some of the PGE concentration (Wang et al., 2008b, 2010).

6.2. Fe-Ti-V oxide-ore deposits

The orthomagmatic Fe-Ti-V oxide deposits of the ELIP are a substantial economic resource. There are at least five world-class magmatic oxide deposits within the Panxi region of the inner zone. Zhou et al. (2005) reported ~7% and ~35% of global production of V and Ti respectively is from China with most of the metals originating from the layered gabbroic complexes of the ELIP. Between the Panzhihua, Hongge, Baima and Taihe deposits there is an estimated 2530 Mt of Fe, 680 Mt of Ti and 28.5 Mt of V (Ma et al., 2003; Zhong et al., 2005). The deposits can be divided into two groups based on their compositions and stratigraphy. For example, the deposits at Hongge and Xinjie may have originated from more primitive parental magmas but were certainly subject to open system magmatic processes (i.e. recharge, assimilation) whereas the Panzhihua, Baima and Taihe deposits likely originated from more evolved parental magmas (i.e. basaltic) and were comparatively less influence by open system magmatic process. Furthermore the Panzhihua, Baima and Taihe gabbros are petrogenetically related to isotropic peralkaline quartz-bearing granitoids whereas the others do not appear to be so.

The formation of the Panzhihua, Baima and Taihe gabbro-granitoid-ore complexes, like many aspects of the ELIP, is a highly debated issue. For instance, some considered the gabbro-ore to be exclusive from the formation of the neighboring granitic rocks whereas others suggest they are part of the same intrusion (Shellnutt et al., 2009a, 2011b; Zhong et al., 2009, 2011a; Shellnutt and Jahn, 2010). Furthermore the formation of the actual ore deposit and host gabbro is widely debated as well and may involve a number of magmatic processes such as silicate immiscibility, fractional crystallization, fluxing of CO_2-rich fluids, and have either a basaltic or ultramafic parental magma (Zhou et al., 2005; Zhang et al., 2006a, b, 2009; Ganino et al., 2008, 2013a, b; Pang et al., 2008a, b, 2009, 2010, 2013; Ganino and Arndt, 2009; Shellnutt et al., 2009a, 2011b; Shellnutt and Jahn, 2010; Hou et al., 2012a, b, 2013; Shellnutt and Pang, 2012).

The main geological and geochemical features of each intrusion include: Fe-Ti-V oxide-ore deposits in the lower stratigraphic layers, mineral assemblage (cumulus olivine, clinopyroxene and plagioclase with interstitial titanomagnetite ± apatite ± sulphide minerals), similar isotope composition (i.e. $\varepsilon_{Nd}(t) \approx +2$ to $+4$, $I_{Sr} \approx 0.7045$ to 0.7055, $\varepsilon_{Hf}(t) \approx +7$ to $+10$), LILE (except Ba and Sr)- and HFSE-(except Eu) depletion and are temporally and spatially associated with peralkaline quartz granitoids. The major features of the three gabbroic intrusions are similar enough to suggest that they underwent similar processes of formation although each intrusion undoubtedly had some unique developments that are more of a function of initial parental magma composition and location of emplacement.

Some of the issues regarding the genesis of the gabbros are easier to explain. The variability of mineral chemistry and zonal nature of each intrusion suggests that they represent open system magma chambers and that multiple magma pulses occurred but they could not be completely open as there is relative isotope homogeneity indicating magma homogenization likely occurred (Pang et al., 2009, 2010, 2013; Shellnutt et al., 2011b; Shellnutt and Pang, 2012; Song et al., 2013). Pang et al. (2009) identified that there is a Zr-depletion problem with the cumulate gabbros. In other words the gabbroic intrusions are too poor in bulk Zr, and other HFSE, to represent a parental magma composition unless an evolved residual liquid was removed. The geochemical, temporal, spatial and the isotopic similarity between the neighboring peralkaline granitic rocks and the cumulate gabbros is very strong evidence that there is a petrogenetic link between the rock types and that they are part of the same igneous complexes (Shellnutt and Zhou, 2007; Shellnutt et al., 2009a, 2011b; Shellnutt and Jahn, 2010). The original parental liquid for the gabbroic intrusions is largely speculative because the chilled margins are not commonly exposed or have been modified by magma-country rock interactions. In most cases the parental liquids are considered to be ‘high-Ti’ Emeishan basalt (Table 3). It is thought that the gabbros are derived from ‘high-Ti’ Emeishan basalt because of the evolved compositions of the olivine (e.g. $<Fo_{82}$) and clinopyroxene (e.g. $Mg^{\#} < 80$) and the trace element budget. Simply stated, if the original parental magma equals the gabbro plus the ore body plus the granitic rocks at various proportions the bulk composition must be basaltic due to the low forsterite values of the olivine and the HFSE budget (Zhou et al., 2005; Pang et al., 2008a, b, 2009; Shellnutt et al., 2009a, b, 2011a, b, c; Zhang et al., 2009; Shellnutt and Jahn, 2010). Consequently, an ultramafic (i.e. ferropicrite) parental magma is not likely suitable for the layered gabbroic intrusions (i.e. Panzhihua, Baima, Taihe) but is probably more likely for the layered mafic-ultramafic intrusions (i.e. Xinjie, Limahe, Hongge), although the basaltic magma may have formed from an ultramafic parental liquid. The more intriguing issues are related to the ore body formation.

The oxide-ore deposits in the gabbros are considered to be related to one or more of silicate immiscibility or CO_2-fluid fluxing to induce oxygen enrichment or crystallization (Zhou et al., 2005; Ganino et al., 2008, 2013a, b; Shellnutt et al., 2011b; Zhou et al., 2013). Silicate immiscibility is thought to be a possible rock forming process where a ferrous (i.e. Fe-rich basalts) silicate liquid will separate from a siliceous (i.e. granitic) silicate liquid (Philpotts, 1976, 1982; Charlier and Grove, 2012). Zhou et al. (2005, 2013) suggested that the oxide-ore zone of the Panzhihua-type gabbros formed by immiscibility where the oxides crystallized from the ferrous silicate liquid and segregated out form the ore deposits. Although silicate immiscibility can occur in terrestrial rocks, it seems that it is not a major magma/rock forming process as the definitive evidence is usually identified from melt inclusions on the order of micron scale (Watson, 1976; Veksler et al., 2006, 2007). Furthermore the necessity to invoke immiscible separation to form oxide minerals and concentrate them into an ore deposit is in conflict with the interstitial titanomagnetite textures. After crystallization of olivine, plagioclase and clinopyroxene, the residual liquid composition from an original high-Ti basaltic parental magma will be enriched in Fe, Ti and incompatible elements and therefore will start to crystallized titanomagnetite in abundance. It could be said that the Fe-Ti-HFSE-rich residual liquid resembles a ferrous silicate liquid but in of itself did not necessarily formed by silicate immiscibility. Additionally the trace element partitioning of silicate immiscibility seems to be at odds as the ferrous silicate liquid will be enriched in incompatible elements as compared with the siliceous liquid (Watson, 1976; Veksler et al., 2006). The fact the contemporaneous, incompatible element-enriched, Mg-Ti-Ba-Sr-Eu-depleted peralkaline quartz granitic rocks are located a few hundred metres away from the cumulate gabbros is rather compelling evidence that they represent the residual liquids after fractional crystallization of a mafic parental magma. The same geological and geochemical relationship is true for the Baima and Taihe intrusions.

Ganino et al. (2008, 2013a, b) have suggested that the release of CO_2-rich fluids from the adjacent Sinian marbles allowed the host magma to be even more oxidizing and contributed to the *en masse* crystallization of titanomagnetite in the Panzhihua intrusion and the formation of the oxide-ore deposit. There is little doubt that the

Table 3
Estimates for the parental magma compositions of the Fe-Ti-V oxide-bearing layered mafic-ultramafic intrusions.

Intrusion	Panzhihua[a]	Panzhihua[b]	Hongge/Panzhihua[c]	Hongge[d]	Xinjie[d]	Taihe[b]	Baima[b]
SiO_2 (wt.%)	42.6	49.18	45.83	47.28	46.24	50.45	44.64
TiO_2	3.99	2.94	4.85	3.51	3.08	2.61	3.48
Al_2O_3	15.8	11.53	15.62	9.93	8.69	12.36	13.79
$Fe_2O_3^t$		12.67				12.19	16.41
FeO^t	15.6			14.41	14.5		
FeO			11.36				
Fe_2O_3			2.23				
MnO	–	0.19	0.23	0.18	0.19	0.20	0.22
MgO	5.99	8.74	7.18	9.39	13.93	7.44	6.95
CaO	11.9	10.54	7.52	11.22	9.83	9.95	10.18
Na_2O	2.45	2.28	3.26	1.76	1.53	2.61	2.40
K_2O	0.31	1.12	1.41	1.15	1.00	1.41	1.09
P_2O_5	0.69	0.31	0.51	0.29	0.26	0.30	0.35
LOI		0.5				0.5	0.5
Total	99.2	100	100.01	99.12	99.25	100	100
$Mg^{\#}$	46	57.8	53	58	67	54.8	45.6
V (ppm)				385	335		
Cr				890	1505		
Co		54				54	52
Ni		115				115	85
Sr		548				550	780
Nb		30.8				24	31
Ba		498				475	590
Ta		2.1				1.6	1.7

[a] Zhou et al. (2005).
[b] Shellnutt et al. (2011b).
[c] Pang et al. (2008a).
[d] Bai et al. (2012b). $Mg^{\#} = 100*[Mg^{2+}/Mg^{2+}+Fe^{2+}]$ where $FeO^t = 0.8998*Fe_2O_3^t$.

parental magma of the Panzhihua complex interacted with the marble country rock as the contact relationship is exposed and there are xenoliths within the lower part of the intrusion but whether there was enough carbonate-fluid assimilated to directly induce titanomagnetite crystallization is another issue (Zhou et al., 2005; Pang et al., 2008a, b, 2009). Panzhihua may be unique in this respect because there are no carbonate country rocks in the immediate vicinity at Baima and Taihe and therefore questions the need to add CO_2-rich fluids to assist in the formation of the oxide deposits. It is possible that the parental magmas for the Baima and Taihe complexes passed through carbonate rocks before they were emplaced but there is no evidence for it at the moment. There is also the issue with the oxidation state of the neighboring granitic rocks. The Panzhihua and Taihe peralkaline granites have a mineral assemblage (i.e. aenigmatite and ilmenite) indicative of reducing oxidation conditions whereas the Baima peralkaline syenite has an oxidizing assemblage (i.e. magnetite, quartz and titanite) (Shellnutt and Iizuka, 2011). The oxidation conditions of a magma are by no means fixed and will change during crystallization and thus conditions of the granites may be different from the gabbros but if O-enrichment through fluxing by CO_2-rich fluids is necessary to invoke oxide-ore formation then why are the Panzhihua and Taihe granites forming under reducing conditions if they are the residual liquids? If it is simply because that by the time the residual silicic liquid formed in Panzhihua and Taihe, the magma was relatively 'depleted' in oxygen then why is the Baima syenite mineralogy indicative of oxidized conditions since there is no evidence for CO_2-fluid fluxing? Furthermore the development of oxide-rich layers in the Xinjie and Hongge intrusions does not appear to require CO_2 fluxing (Zhong et al., 2003, 2004). The necessity of CO_2-fluid fluxing for the formation of the oxide-ore deposits is uncertain because it seems, with respect to the Baima, Taihe, Xinjie and Hongge complexes, oxide-ore deposits would form nevertheless and that the fluxing may simply accelerate the oxide crystallization process.

One process which is consistently mentioned with respect to the Panzhihua, Baima and Taihe complexes is fractional crystallization (Zhou et al., 2005; Ganino et al., 2008; Pang et al., 2008a, b, 2009, 2010, 2013; Shellnutt et al., 2009a, 2011b; Zhang et al., 2009; Shellnutt and Jahn, 2010; Zhong et al., 2011a; Hou et al., 2012a; Shellnutt and Pang, 2012; Song et al., 2013). As mentioned previously, there is evidence for open system behavior and internal redistribution of crystals but the overall process which is affecting the magma system is crystallization and the consequences of an evolving magma, specifically the major and trace element budget, rather than assimilation, contamination or unusual magma type. The discussion on immiscibility highlighted the fact that the trace element budget of the layered gabbros is not sufficiently accounted for unless a residual liquid is considered (Pang et al., 2009). The obvious candidate for the residual liquid is the neighboring peralkaline granitic rocks (Shellnutt et al., 2011b). In each complex there are intermediate (e.g. syenodiorite) composition rocks either as a 'transitional' plutonic body, in the case of Panzhihua, or as microgranular enclaves, in the case of Baima and Taihe (Shellnutt and Jahn, 2010; Shellnutt et al., 2010). The overarching premise is that a basaltic parental magma as represented by a 'high-Ti' Emeishan basalt is injected in the shallow crust and crystallizes olivine, plagioclase and clinopyroxene (Fig. 10). Titanomagnetite will crystallize as soon as conditions permit but the net result will be that the residual liquid composition becomes more silicic (Shellnutt and Zhou, 2007; Shellnutt et al., 2011b). Assimilation of CO_2-rich fluids or other crustal material and/or internal redistribution may or may not be necessary to form the deposits but it is unlikely that the parental magma was picritic.

6.3. Potential of rare earth element deposits

The Panxi region of the Emeishan large igneous province, specifically from Mianning to Dechang, is one of the richest REE-deposit areas of southwestern China. There are numerous Eocene

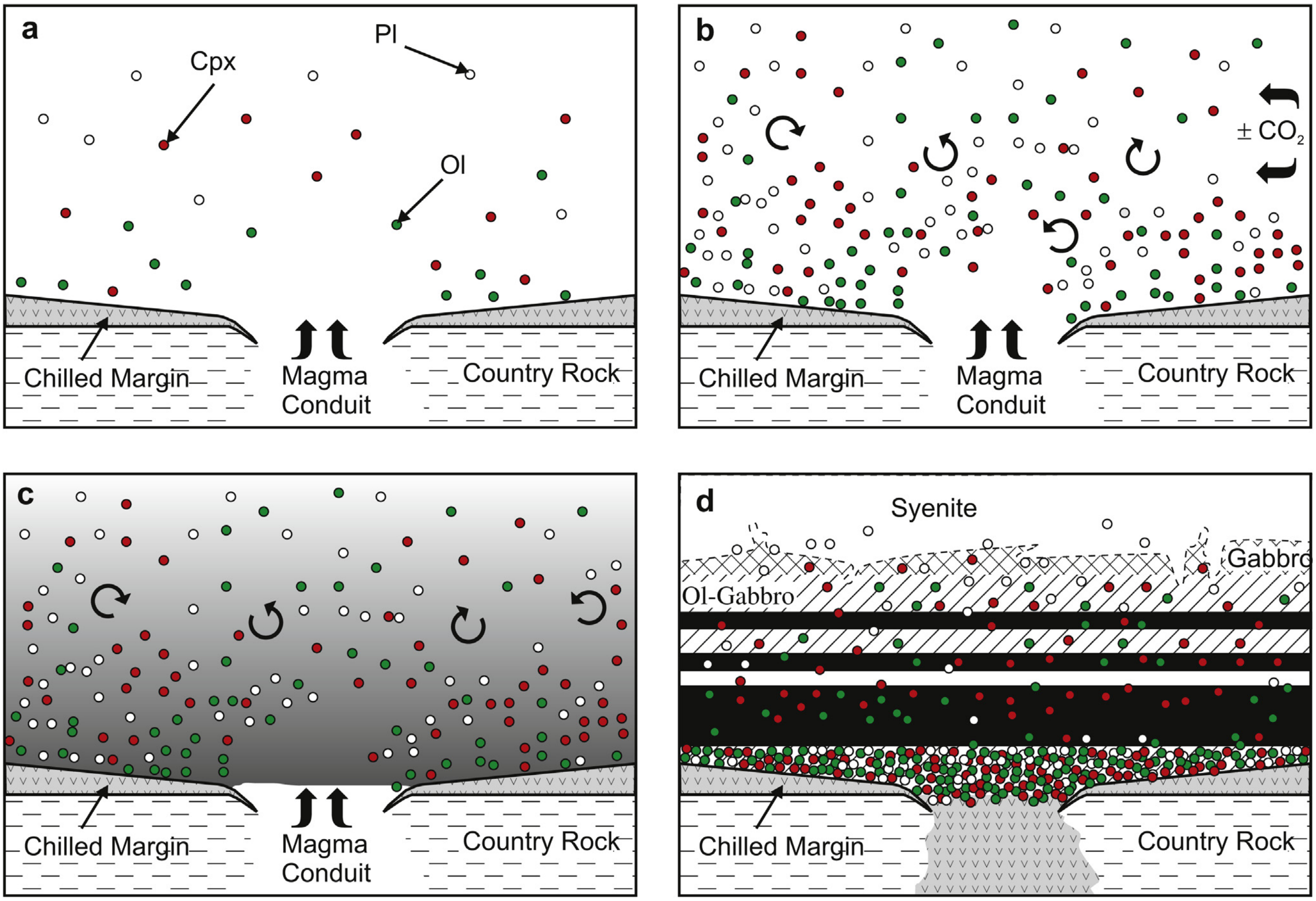

Figure 10. Proposed petrogenetic model of the formation of the Panzhihua, Baima and Taihe magmatic Fe-Ti-V oxide-bearing layered intrusions. (a) Emplacement of a parental magma resembling a Ti-rich Emeishan basalt with an initial amount of suspended crystals. (b) Settling and *in situ* crystallization of cumulate olivine, plagioclase and clinopyroxene with possible fluxing of CO_2 from the surrounding country rocks. Additional magmas may or may not be injected. (c) After a period of fractionation, a lighter alkali-rich (white) residual magma migrates to the top of the magma chamber. At this point the magma chamber is likely oxygenated and crystallizes massive amounts of magnetite (black) in the lower part of the magma chamber while the silicic liquid forms in the upper part of the magma chamber. (d) Solidification and stratification of the BIC gabbroic unit into four zones and formation of the granitic rocks.

(40 Ma) to Miocene (10 Ma) alkalic-granite/syenite and carbonatitic plutons throughout this region some of which (e.g. Maoniuping) contain significant REE mineralization (Niu et al., 2003; Hou et al., 2009; Xu et al., 2012). The common mineral assemblage within the Eocene to Miocene granites includes bastnasite, fluorite, barite and aegirine-augite. The Mianning-Dechang alkalic granites and syenites share many chemical characteristics with the alkalic granitoids from western Mongolia and the ELIP in particular the peralkaline rocks (Kovalenko et al., 1995; Shellnutt and Zhou, 2007; Hou et al., 2009). Currently, there are few, if any, REE-deposit directly associated with the alkalic granitoids of the ELIP however their mineral assemblages suggest there may be potential for mineralization either as hydrothermal-magmatic or as depositional deposits (Niu et al., 2003).

The abundance of HFSE in the ELIP peralkaline granitoids (i.e. Panzhihua, Baima, Taihe) is known to be as high 0.3 wt.% and the host rocks contain REE-ore minerals (i.e. bastnasite). The plutons, both metaluminous and peralkaline, of the ELIP were intruded by high temperature mafic dykes which were likely hot enough to induce partial melting and remobilization of REEs within the peralkaline rocks and thus could create economic concentrations similar to magmatic-hydrothermal deposits (Shellnutt et al., 2008). Alternatively, and perhaps more likely, late stage magmatic fluids derived from the alkaline granitoids could have concentrated the HFSE and formed enriched-veins or veinlets of REE-rich minerals (Salvi and Williams-Jones, 2005). The identification of magmatic chevkinite within the Woshui metaluminous pluton suggests there could be another type of REE-deposit in the region (Shellnutt and Iizuka, 2013). Although the Woshui pluton was also intruded by mafic dykes, the bulk REE content is likely to be too low for economic concentrations but there remains a possibility that eroded material from the pluton could accumulate in the neighboring basins and valleys and be a potential for ion-adsorption clay deposits. In addition to the detritus from the Woshui pluton, material from the Baima pluton could also be added and possibly increase the likelihood REE-rich material could be deposited (van Olphen, 1959; Kanazawa and Kamitani, 2006; Bao and Zhao, 2008). Therefore the alkalic rocks of the ELIP are a potential target for magmatic-hydrothermal deposits or they may have acted as a source for possible ion-adsorption clay deposits.

7. Tectonomagmatic synthesis of the Emeishan large igneous province

A unifying theory of the formation of the ELIP is a difficult issue to address because the available data and geological evidence dictate that some studies are more likely to be correct than other studies. For example the range of Sr-Nd-Pb-Os isotopes of Emeishan rocks does not permit any resounding conclusion on the type of mantle source and therefore it could be said that a sub-lithospheric mantle source, or a subcontinental lithospheric mantle source or both are involved. Furthermore the effects of crustal contamination can mask the features of the original mantle source. This section brings together the main geological and geochemical features of the ELIP in order to constrain its likely tectonomagmatic history.

During the late Capitanian to early Wuchiapingian the Yangtze Block was a stable carbonate platform at tropical latitudes. It is uncertain what the topography (i.e. flat or undulatory) of the carbonate platform was but the modern day Mascarene Plateau may be a good analog because it is possible that some portion of the Yangtze Block was exposed whereas most of the platform was submerged. The Emeishan volcanic rocks erupted along with formation of several plutonic complexes. Huang and Opdyke (1998), Thompson et al. (2001) and He et al. (2003, 2007) suggested that volcanism was short-lived, probably within one magnetic reversal cycle or <3 Ma (Ali et al., 2005; Zheng et al., 2010; Shellnutt et al., 2012a). A short duration is consistent with eruption rates and emplacement models for many large igneous provinces (Coffin and Eldholm, 1994; Bryan and Ernst, 2008). Age dates and correlations of mafic and acidic layers near the Permo-Triassic boundary of Southwest China have suggested that the ELIP may have extended beyond the late Permian but is not likely a part of the main effusive period (Fan et al., 2004; Kamo et al., 2006). It is unlikely that ELIP magmatism was continuously active for ~20 Ma as CA-ID-TIMS results show that some of the rocks previously dated at ~252 Ma are in fact ~259 Ma (Shellnutt et al., 2012a). Verification of the late Permian ages (i.e. 252 Ma) and Triassic ages (i.e. 240 Ma) is required but it is possible that underplated mafic rocks related to the ELIP served as a source for post-260 Ma magmas.

The volcanic and the plutonic rocks are likely derived from magmas generated from a mantle plume source (Fig. 11). Some magmas were subsequently contaminated by various amounts of crustal material. The major and trace elemental and isotope composition of the Emeishan magmatic rocks indicate that the source was heterogeneous and possibly volatile-rich as is the case for some Ti-rich basaltic rocks (Pilet et al., 2005, 2008). The subcontinental lithospheric mantle may or may not be involved but probably cannot be discerned with ease due to the isotopic heterogeneity of the rocks and the fact that the source may have been volatile-rich (e.g. CO_2, F) and contaminated with crustal material (e.g. GLOSS). The volatiles could be from the original source or mixing within an enriched component (i.e. GLOSS) or simply due to low amount of partial melting. Whether uplift and doming of the crust occurred is not a prerequisite for the formation of the flood basalts and may or may not have occurred (He et al., 2003, 2007, 2010a, b; Utskins-Peate and Bryan, 2008; Ali et al., 2010; Sun et al., 2010). The injection of mafic magmas induced partial melting of the Yangtze Block which led to the formation of the peraluminous to metaluminous silicic rocks whereas mingling between mafic magmas and crustal melts produced other metaluminous silicic rocks (Shellnutt et al., 2011c). The mafic magmas which did not erupt but reached shallow crustal levels (i.e. <3 km) crystallized and formed the cumulate layered mafic-ultramafic complexes some of which produced both volcanic and plutonic peralkaline silicic rocks (Fig. 11). The formation of ore deposits within the layered intrusions is dependent on the depth of emplacement, the original parental magma composition, amount and timing of crustal assimilation including country rock volatile fluxing. It is possible, providing that magmatism was short-lived,

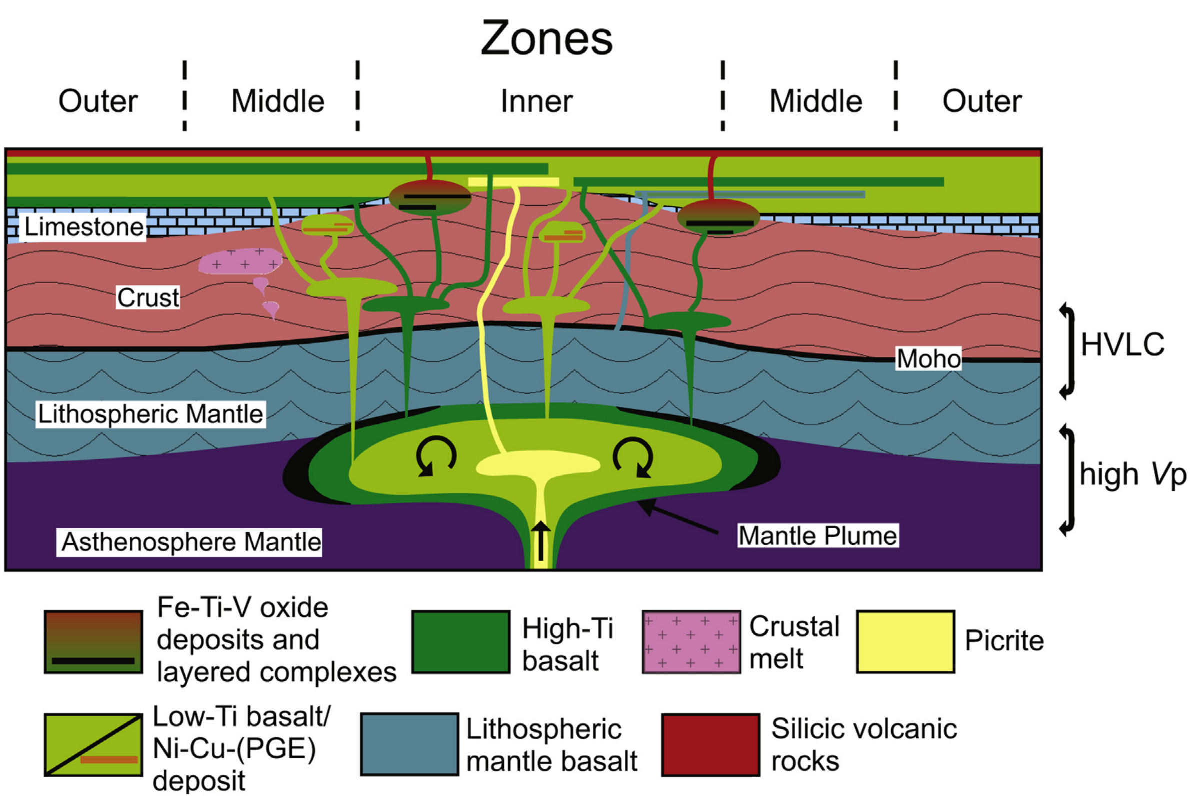

Figure 11. At 260 Ma the ELIP plume head arrives at the base of the lithosphere possibly inducing uplift of the crust and decompressional melting of the plume source. Mafic magmas are injected into the lower crust/upper mantle forming chambers and the HVLC layer. Some magmas erupt onto the surface whereas others reach relatively shallow depths and form the oxide-ore bearing layered intrusions and sulphide ore bearing intrusions. The continuous injection of mafic magmas likely induced partial melting of the crust which leads to the formation of the crust-derived silicic plutons and possible the hybrid silicic plutons.

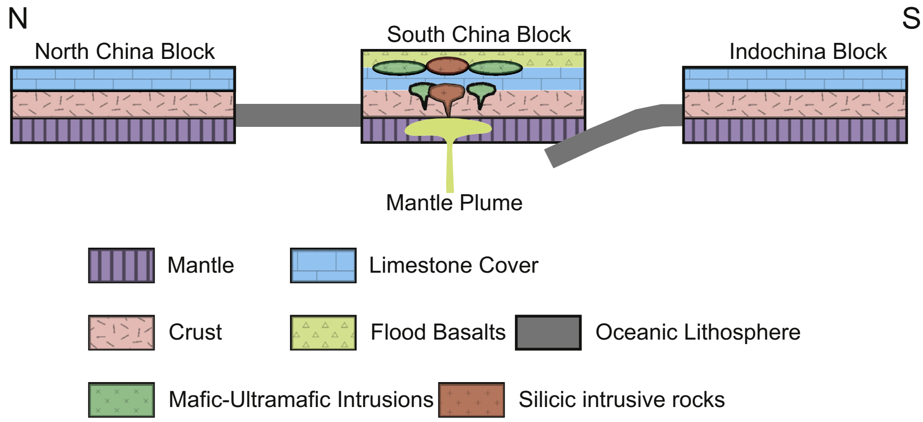

Figure 12. A simplified block model of the regional tectonic positions of the North China Block and Indochina Block to the South China Block during the emplacement of the ELIP (260 Ma).

that country rock degassing contributed to climatic changes which adversely affected global ecosystems.

The cause of the ELIP is uncertain. It could simply be due to the random formation of a mantle plume related to global plate tectonics or it could be due to the plate dynamics of the North China-South China-Indochina Block (Fig. 12) (Shellnutt et al., 2008; Jian et al., 2009). The current location of the Panxi region is along a marginal boundary between the Yangtze Block and the Songpan-Ganze terrain of the Tibetan Plateau and does not correspond with an intra-plate setting. The composition of basaltic and A-type granitic rocks has long been used as evidence for within plate mafic magmatism (c.f. Pearce and Cann, 1973; Pearce et al., 1984). The composition of the Panxi plutons and the mafic dykes are consistent with a rifting environment or within plate setting. The geological evidence is a little more complicated due to Mesozoic to Cenozoic tectonic over printing in SW China. After emplacement of the ELIP, which undoubtedly was a within plate extensional setting (He et al., 2003; Xu et al., 2004), the SCB moved northward into Eurasia around 231 Ma which caused widespread deformation of the western margin of the Yangtze Block thereby destroying the outer margin and creating an appearance of a margin setting of the modern ELIP (Fig. 12) (Bruguier et al., 1997). Many LIPs are associated with continental break-up and mantle plumes (Coffin and Eldholm, 1994; Courtillot et al., 1999; Ernst et al., 2005) but not all are related to both (Sheth, 1999, 2005a, b; McHone, 2000). The emplacement of the ELIP was tensional however it was unlikely to have caused the Yangtze Block to split. This presents an interesting problem and leads to the question: did the Yangtze Block split? Considering that many continental break-ups occur along plate margins or suture zones it is suggested that the location of the Emeishan mantle plume was not concomitant with a major lithospheric inhomogeneity (i.e. a plate margin or tectonic suture zone) (Courtillot et al., 1999). Also, the impending collision between the NCB and the SCB may have prevented complete plate break-up as the extended plate would have simply been pushed back together upon collision. It is generally agreed that the majority of Emeishan flood basalts erupted within a short period around 260 Ma so it is likely that ELIP-related extension stopped shortly thereafter.

8. Future directions

Considering the amount of research that has been published over the past 20 years on the ELIP, the question is: where do we go from here? In my opinion there is plenty of whole rock, major and trace elemental data, isotope data and paleomagnetic studies to constrain the formation of the ELIP and that additional geochemical studies may not change the overall state of knowledge. Furthermore, the evidence for uplift and doming of the crust prior to the eruption of the Emeishan basalts may be debated in literature continuously and is beginning to resemble scientific 'trench-warfare' where enormous amounts of energy and capital are invested into solving the problem but the advancement in knowledge will be minimal and, most importantly, the probability of a breakthrough will be low. However the identification of mantle plumes and their consequences is a first order geoscience problem and thus the ELIP may be a 'frontline' region to examine or test mantle plume theory for years to come.

I believe studies on the ELIP should focus on refinement and detailed investigations of magma-scale or mineral-scale issues. Microanalytical techniques applied to mineral/melt inclusions of accessory minerals (e.g. apatite, fluorite) may provide evidence for the original parental compositions of some of the plutonic rocks or possibly highlight some of the processes which are ongoing during crystallization or ore formation. The poor age precision on the emplacement of the ELIP must be refined. Current *in situ* zircon U-Pb techniques provide 'good enough' results but require better precision and thus CA-ID-TIMS mineral (i.e. zircon or baddeleyite) could be applied to constrain the duration of magmatism more precisely. Specifically the latest Permian and Triassic ages of 'ELIP-related' rocks must be verified. If the younger ELIP ages are verified then it would be evidence in support of long-lived magmatism and a time progression feature similar to the Hawaiian Islands-Emperor seamount chain.

I believe more detailed work must be done on the ore deposits and exploration of new types of deposits. In an ideal world this would mean new drilling and cooperation between publically funded researchers and private or state-owned companies. Some sites, like Panzhihua are wonderfully exposed but Taihe and Baima are not or at least not yet and there are other areas where a drill core may provide value insight and possibly a new deposit. Finally, I think it would be worthwhile to examine the possibility of REE-deposits associated with the alkaline granitic rocks. If new ideas and challenges are not met then ELIP research will become mundane and inconsequential. Because of the excellent exposure of the ELIP plumbing system there is an opportunity to find new information on how LIPs and their magmatic systems develop which will have tremendous implications for petrology, economic geology and mantle plume theory.

Acknowledgments

I would like to thank an anonymous reviewer and M. Santosh for constructive comments on the manuscript and Jarda Dostal for reviewing an earlier version of the manuscript. Special thanks to Mei-Fu Zhou for introducing me to the ELIP and Jason Ali, Sun-Lin Chung, Clement Ganino, Eero Hanski, Bor-Ming Jahn, George Ma, Kwan-Nang Pang, Liang Qi, Xie-Yan Song, Christina Wang, Kuo-Lung Wang and Yi-Gang Xu for very enlightening discussions on a variety of ELIP-related topics over the years. This project was supported by NSC grant 102-2628-M-003-001-MY4 to JGS.

References

Albarede, F., 1992. How deep do common basaltic magmas form and differentiate. Journal of Geophysical Research 97, 10997–11009.
Ali, J.R., Fitton, J.G., Herzberg, C., 2010. Emeishan large igneous province (SW China) and the mantle-plume up-doming hypothesis. Journal of the Geological Society 167, 953–959.
Ali, J.R., Thompson, G.M., Zhou, M.-F., Song, X.Y., 2005. Emeishan large igneous province, SW China. Lithos 79, 475–489.
Ali, J.R., Lo, C.-H., Thompson, G.M., Song, X.Y., 2004. Emeishan basalt Ar-Ar overprint ages define several tectonic events that affected the western Yangtze platform in the Mesozoic Cenozoic. Journal of Asian Earth Science 23, 163–178.
Ali, J.R., Thompson, G.M., Song, X.-Y., Wang, Y., 2002. Emeishan basalts (SW China) and the 'end-Guadalupian' crisis: magnetobiostratigraphic constraints. Journal of the Geological Society London 159, 21–29.
Anh, T.V., Pang, K.-N., Chung, S.-L., H.-M., Hoa, T.T., Anh, T.T., Yang, H.-J., 2011. The Song Da magmatic suite revisited: a petrologic, geochemical and Sr–Nd isotopic study on picrites, flood basalts and silicic volcanic rocks. Journal of Asian Earth Sciences 42, 1341–1355.
Bai, Z.-J., Zhong, H., Li, C., Zhu, W.-G., Xu, G.-W., 2012a. Platinum-group elements in the oxide layers of the Hongge mafic–ultramafic intrusion, Emeishan Large Igneous Province, SW China. Ore Geology Reviews 46, 149–161.
Bai, Z.-J., Zhong, H., Naldrett, A.J., Zhu, W.-G., Xu, G.-W., 2012b. Whole-rock and mineral composition constraints on the genesis of the giant Hongge Fe-Ti-V oxide deposit in the Emeishan large igneous province, southwest China. Economic Geology 107, 507–524.
Baksi, A.K., 2001. Search for a deep-mantle component in mafic lavas using a Nb-Y-Zr plot. Canadian Journal of Earth Sciences 38, 813–824.
Bao, Z., Zhao, Z., 2008. Geochemistry of mineralization with exchangeable REY in the weathering crusts of granitic rocks in South China. Ore Geology Reviews 33, 519–535.
Borisenko, A.S., Sotnikov, V.I., Izokh, A.E., Polyakov, G.V., Obolensky, A.A., 2006. Permo-Triassic mineralization in Asia and its relation to plume magmatism. Russian Geology and Geophysics 47, 166–182.
Boven, A., Pasteels, P., Punzalan, L.E., Liu, J., Luo, X., Zhang, W., Guo, Z., Hertogen, J., 2002. $^{40}Ar/^{39}Ar$ geochronological constraints on the age and evolution of the Permo-Triassic Emeishan volcanic province, southwest China. Journal of Asian Earth Sciences 20, 157–175.
Brozdowski, R.A., Page, M.L., Zang, W., Dong, Q.J., 2004. Jinbaoshan (JBS) Pt-Pd-Ni-Cu deposit, Yunnan, P.R. China. In: Shellnutt, J.G., Zhou, M.-F., Pang, K.-N. (Eds.), Proceedings of the IGCP 479 Hong Kong Workshop: Recent Advances in Magmatic Ore Systems in Mafic-ultramafic Rocks, pp. 67–69. Abstract Volume.
Bruguier, O., Lancelot, J.R., Malavieille, J., 1997. U–Pb dating on single detrital zircon grains from the Triassic Songpan–Ganze flysch Central China: provenance and tectonic correlations. Earth and Planetary Science Letters 152, 217–231.
Bryan, S.E., Ernst, R.E., 2008. Revised definition of large igneous provinces (LIPs). Earth-Science Reviews 86, 175–202.
Burov, E., Guillou-Frottier, L., 2005. The plume head-continental lithosphere interaction using a tectonically realistic formulation for the lithosphere. Geophysical Journal International 161, 469–490.
Campbell, I.H., 2007. Testing the plume theory. Chemical Geology 241, 153–176.
Campbell, I.H., 2005. Large igneous provinces and the mantle plume hypothesis. Elements 1, 265–269.
Campbell, I.H., Griffiths, R.W., 1990. Implications of mantle plume structure for the evolution of flood basalts. Earth and Planetary Science Letters 99, 79–93.
Charlier, B., Grove, T.L., 2012. Experiments on liquid immiscibility along tholeiitic lines of descent. Contributions to Mineralogy and Petrology 164, 27–44.
Chauvel, C., Lewin, E., Carpenter, M., Arndt, N.T., Marini, J.-C., 2008. Role of the recycled oceanic basalt and sediment in generating the Hf-Nd mantle array. Nature Geoscience 1, 64–67.
Chen, J., Jahn, B.-M., 1998. Crustal evolution of southeastern China: Nd and Sr isotopic evidence. Tectonophysics 284, 101–133.
Chen, J., Yang, X., Xiao, L., He, Q., 2010. Coupling of basaltic magma evolution and lithospheric seismic structure in the Emeishan large igneous province: MELTS modeling constraints. Lithos 119, 61–74.
Chung, S.-L., Jahn, B.-M., 1995. Plume-lithosphere interaction in generation of the Emeishan flood basalts at the Permian-Triassic boundary. Geology 23, 889–892.
Chung, S.-L., Jahn, B.-M., Genyao, W., Lo, C.H., Bolin, C., 1998. The Emeishan flood basalt in SW China: a mantle plume initiation model and its connection with continental breakup and mass extinction at the Permian-Triassic boundary. In: Flower, M.F.J., Chung, S.-L., Lo, C.H., Lee, T.Y. (Eds.), Mantle Dynamics and Plate Interactions in East Asia, American Geophysical Union Geodynamic Series, vol. 27, pp. 47–58.
Chung, S.-L., Lee, T.-Y., Lo, C.-H., Wang, P.-L., Chen, C.-Y., Yem, N.T., Hoa, T.T., Genyao, W., 1997. Intraplate extension prior to continental extrusion along the Ailao Shan-Red River shear zone. Geology 25, 311–314.
Cliff, R.A., Baker, P.E., Mateer, N.J., 1991. Geochemistry of inaccessible island volcanics. Chemical Geology 92, 251–260.
Coffin, M.F., Eldholm, O., 2001. Large Igneous Provinces: progenitors of some ophiolites?. In: Ernst, R.E., Buchan, K.L. (Eds.), Mantle Plumes: Their Identification through Time, vol. 352 Geological Society of America, pp. 59–70. Special Paper.
Coffin, M.F., Eldholm, O., 1994. Large igneous provinces: crustal structure, dimensions and external consequences. Reviews in Geophysics 32, 1–36.
Courtillot, V.E., Renne, P.R., 2003. On the ages of flood basalt events. Comptes Rendus Geoscience 335, 113–140.
Courtillot, V., Jaupart, C., Manighetti, I., Tapponier, P., Besse, J., 1999. On causal links between flood basalts and continental breakup. Earth and Planetary Science Letters 166, 177–195.
Cox, K.G., 1989. The role of mantle plumes in the development of continental drainage patterns. Nature 342, 873–877.
Elkins-Tanton, L.T., 2007. Continental magmatism volatile recycling, and a heterogeneous mantle caused by lithospheric gravitational instabilities. Journal of Geophysical Research 112, B03405. http://dx.doi.org/10.1029/2005JB004072.
Ernst, R.E., 2007. Large igneous provinces in Canada through time and their metallogenic potential. In: Goodfellow, W.D. (Ed.), Mineral Deposits of Canada: a Synthesis of Major Deposit-types, District Metallogeny, the Evolution of Geological Provinces, and Exploration Methods, 5. Geological Association of Canada, Mineral Deposits Division, pp. 929–937. Special Publication.
Ernst, R.E., Buchan, K.L., Campbell, I.H., 2005. Frontiers in large igneous province research. Lithos 79, 271–297.
Ernst, R.E., Buchan, K.L., 2003. Recognizing mantle plumes in the geological record. Annual Review of Earth and Planetary Sciences 31, 469–523.
Fan, W., Zhang, C., Wang, Y., Guo, F., Peng, T., 2008. Geochronology and geochemistry of Permian basalts in western Guangxi Province, southwest China: evidence for plume-lithosphere interaction. Lithos 102, 218–236.
Fan, W., Wang, V., Peng, T., Miao, L., Guo, F., 2004. Ar-Ar and U-Pb geochronology of late Paleozoic basalts in western Guangxi and its constraints on the eruption age of Emeishan basalt magmatism. Chinese Science Bulletin 49, 2318–2327.
Farnetani, C.G., Richards, M.A., 1994. Numerical investigations of the mantle plume initiation model for flood basalt events. Journal of Geophysical Research 99, 13813–13833.
Favela, J., Anderson, D.L., 2000. Extensional tectonics and global volcanism. In: Boschi, E., Ekstrom, G., Morelli, A. (Eds.), Problems in Geophysics for the New Millennium. Editrice Compositori, Bologna, Italy, pp. 463–498.
Fitton, J.G., Saunders, A.D., Norry, M.J., Hardarson, B.S., Taylor, R.N., 1997. Thermal and chemical structure of the Iceland plume. Earth and Planetary Science Letters 153, 197–208.
Foulger, G.R., 2010. Plates vs Plumes: a Geological Controversy. Wiley-Blackwell, Chichester, 328 pp.
Ganino, C., Harris, C., Arndt, N.T., Prevec, S.A., Howarth, G.H., 2013a. Assimilation of carbonate country rock by the parent magma of the Panzhihua Fe-Ti-V deposit (SW China): evidence from stable isotopes. Geoscience Frontiers 4, 547–554.
Ganino, C., Arndt, N.T., Chauvel, C., Alexandre, J., Athurion, C., 2013b. Melting of carbonate wall rocks and formation of the heterogeneous aureole of the Panzhihua intrusion, China. Geoscience Frontiers 4, 535–546.
Ganino, C., Arndt, N.T., 2009. Climate changes caused by degassing of sediments during the emplacement of large igneous province. Geology 37, 323–326.
Ganino, C., Arndt, N.T., Zhou, M.-F., Gaillard, F., Chauvel, C., 2008. Interaction of magma with sedimentary wall rock and magnetite ore genesis in the Panzhihua mafic intrusion. SW China. Mineralium Deposita 43, 677–694.
Glazner, A.F., 2007. Thermal limitations on incorporation of wall rock into magma. Geology 35, 319–322.
Glotov, A.I., Polyakov, G.V., Hoa, Tran Trong, Balykin, P.A., Akimtsev, V.R., Krivenko, A.P., Tolstykh, N.D., Phuong, Ngo Thi, Thanh, Hoang Huu, Hung, Tran Quoz, Petrova, T.E., 2001. The Ban Phuc Ni-Cu-PGE deposit related to the Phanerozoic komatiite basalt association in the Song Da rift, northwestern Vietnam. Canadian Mineralogist 39, 573–589.
Gradstein, F.M., Ogg, J.G., Smith, A.G. (Eds.), 2004. A Geologic Time Scale. Cambridge University Press, Cambridge, 589 pp.
Griffiths, R.W., Campbell, I.H., 1991. Interaction of mantle plume heads with the Earth's surface and onset of small scale convection. Journal of Geophysical Research 96, 295–310.
Guo, F., Fan, W., Wang, Y., Li, C., 2004. When did the Emeishan mantle plume activity start? Geochronological and geochemical evidence from ultramafic-mafic dikes in southwestern China. International Geology Review 46, 226–234.
Hanski, E., Kamenetsky, V.S., Luo, Z.-Y., Xu, Y.-G., Kuzmin, D.V., 2010. Primitive magmas in the Emeishan large igneous province, southwestern China and northern Vietnam. Lithos 119, 75–90.
Hanski, E., Walker, R.J., Huhma, H., Polyakov, G.V., Balykin, P.A., Hoa, T.T., Phuong, N.T., 2004. Origin of the Permian-Triassic komatiites, northwestern Vietnam. Contributions to Mineralogy and Petrology 147, 453–469.
Hao, Y., Zhang, Z., Wang, F., Mahoney, J.J., 2004. Petrogenesis of high-Ti and low-Ti basalts from the Emeishan large igneous province. Geological Review 50, 587–592 (in Chinese).
Haq, B.U., Schutter, S.R., 2008. A chronology of Paleozoic sea-level changes. Science 322, 64–68.
Hart, S.R., Hauri, E.H., Oschmann, L.A., Whitehead, J.A., 1992. Mantle plumes and entrainment: isotopic evidence. Science 256, 517–520.

Hawkesworth, C., Scherstein, A., 2007. Mantle plumes and geochemistry. Chemical Geology 241, 319–331.
He, B., Xu, Y.-G., Guan, J.-P., Zhong, Y.-T., 2010a. Paleokarst on the top of the Maokou formation: further evidence for domal crustal uplift prior to the Emeishan flood volcanism. Lithos 119, 1–9.
He, B., Xu, Y.-G., Zhong, Y.-T., Guan, J.-P., 2010b. The Guadalupian-Lopingian boundary mudstones at Chaotian (SW China) are clastic rocks rather than acidic tuffs: implication for a temporal coincidence between the end-Guadalupian mass extinction and the Emeishan volcanism. Lithos 119, 10–19.
He, B., Xu, Y.-G., Huang, X.-L., Luo, Z.-Y., Shi, Y.-R., Yang, O.-J., Yu, S.-Y., 2007. Age and duration of the Emeishan flood volcanism, SW China: geochemistry and SHRIMP zircon U–Pb dating of silicic ignimbrites, post-volcanic Xuanwei formation and clay tuff at the Chaotian section. Earth and Planetary Science Letters 255, 306–323.
He, B., Xu, Y.-G., Chung, S.-L., Xiao, L., Wang, Y., 2003. Sedimentary evidence for a rapid, kilometer-scale crustal doming prior to the eruption of the Emeishan flood basalts. Earth and Planetary Science Letters 213, 391–405.
He, Q., Xiao, L., Balta, B., Gao, R., Chen, J., 2010c. Variety and complexity of the Late-Permian Emeishan basalts: reappraisal of plume-lithosphere interaction processes. Lithos 119, 91–107.
Herzberg, C., Asimow, P.D., 2008. Petrology of some oceanic island basalts: PRIMELT2.XLS software for primary magma calculation. Geochemistry, Geophysics, Geosystems 9, Q09001. http://dx.doi.org/10.1029/2008GC002057.
Herzberg, C., Asimow, P.D., Arndt, N., Niu, Y., Lesher, C.M., Fitton, J.G., Cheadle, M.J., Saunders, A.D., 2007. Temperatures in ambient mantle and plumes: constraints from basalts, picrites, and komatiites. Geochemistry, Geophysics, Geosystems 8, Q02006. http://dx.doi.org/10.1029/2006GC001390.
Herzberg, C., O'Hara, M.J., 2002. Plume-associated ultramafic magmas of Phanerozoic age. Journal of Petrology 43, 1857–1883.
Hou, T., Zhang, Z., Encarnacion, J., Santosh, M., 2012a. Petrogenesis and metallogenesis of the Taihe gabbroic intrusion associated with Fe-Ti-oxide ores in the Panxi district, Emeishan large igneous province southwest, China. Ore Geology Reviews. http://dx.doi.org/10.1016/j.oregeorev.2012.09.004.
Hou, T., Zhang, Z., Pirajno, F., 2012b. A new metallogenic model of the Panzhihua giant V-Ti-iron oxide deposit (Emeishan large igneous province) based on high-Mg olivine-bearing wehrlite and new field evidence. International Geology Review 54, 1721–1745.
Hou, T., Zhang, Z.C., Encarnacion, J., Santosh, M., Sun, Y.L., 2013. The role of recycled oceanic crust in magmatism and metallogeny: Os–Sr–Nd isotopes, U–Pb geochronology and geochemistry of picritic dykes in the Panzhihua giant Fe–Ti oxide deposit, central Emeishan large igneous province, SW China. Contributions to Mineralogy and Petrology 165, 805–822.
Hou, T., Zhang, Z., Kusky, T., Du, Y., Liu, J., Zhao, Z., 2011. A reappraisal of the high-Ti and low-Ti classification of basalts and petrogenetic linkage between basalts and mafic-ultramafic intrusions in the Emeishan large igneous province, SW China. Ore Geology Reviews 41, 133–143.
Hou, Z., Tian, S., Xie, Y., Yang, Z., Yuan, Z., Yin, S., Yi, L., Fei, H., Zou, T., Bai, G., Li, X., 2009. The Himalayan Mianning-Dechang REE belt associated with carbonatite-alkaline complexes, eastern Indo-Asian collision zone, SW China. Ore Geology Reviews 36, 65–89.
Hou, Z.Q., Lu, J.R., Lin, S.Z., 2006. Heterogeneity of a plume axis: bulk-rock geochemical evidence from picrites and basalts in the Emei large igneous province, southwest China. International Geology Review 48, 1087–1112.
Hsu, K.J., Li, J., Chen, H., Wang, Q., Sun, S., Sengor, A.M.C., 1990. Tectonics of south China: key to understanding west Pacific geology. Tectonophysics 183, 9–39.
Huang, K., Opdyke, N.D., 1998. Magnetostratigraphic investigations of an Emeishan basalt section in western Guizhou Province, China. Earth and Planetary Science Letters 163, 1–14.
Huang, K.N., 1986. The Petrological and Geochemical Characteristics of the Emeishan Basalts from SW China and the Tectonic Setting of Their Formation. PhD thesis. Institute of Geology, Academia Sinica (in Chinese).
Jerram, D.A., Widdowson, M., 2005. The anatomy of Continental Flood Basalt Provinces: geological constraints on the processes and products of flood volcanism. Lithos 79, 385–405.
Jian, P., Liu, D., Kroner, A., Zhang, Q., Wang, Y., Sun, X., Zhang, W., 2009. Devonian to Permian plate tectonic cycle of the Paleo-Tethys orogeny in southwest China (II): insights from zircon ages of ophiolites, arc/back-arc assemblages and within-plate igneous rocks and generation of the Emeishan CFB province. Lithos 113, 767–784.
Kamenetsky, V.S., Chung, S.-L., Kamenetsky, M.B., Kuzmin, D.V., 2012. Picrites from the Emeishan large igneous province, SW China: a compositional continuum in primitive magmas and their respective mantle sources. Journal of Petrology 53, 2095–2113.
Kamo, S.L., Crowley, J., Bowring, S.A., 2006. The Permian-Triassic boundary event and eruption of the Siberian flood basalts: an inter-laboratory U–Pb dating study. Geochimica et Cosmochimica Acta 70, A303.
Kanazawa, Y., Kamitani, M., 2006. Rare earth minerals and resources in the world. Journal of Alloys and Compounds 408–412, 1339–1343.
Kovalenko, V.I., Tsaryeva, G.M., Goreglyad, A.V., Yarmolyuk, V.V., Troitsky, V.A., Hervig, R.L., Farmer, G.L., 1995. The peralkaline granite-related Khaldzan-Buregtey rare metal (Zr, Nb, REE) deposit, western Mongolia. Economic Geology 90, 530–547.
Lai, S., Qin, J., Li, Y., Li, S., Santosh, M., 2012. Permian high Ti/Y basalt from the eastern part of the Emeishan large igneous province, southwestern China: petrogenesis and tectonic implications. Journal of Asian Earth Sciences 47, 216–230.
Li, C., Tao, Y., Qi, L., Ripley, E.M., 2012. Controls on PGE fractionation in the Emeishan picrites and basalts: constraints from integrated lithophile–siderophile elements and Sr–Nd isotopes. Geochimica et Cosmochimica Acta 90, 12–32.
Li, J., Xu, J.-F., Suzuki, K., He, B., Xu, Y.-G., Ren, Z.-Y., 2010. Os, Nd and Sr isotope and trace element geochemistry of the Muli picrites: insights into the mantle source of the Emeishan large igneous province. Lithos 119, 108–122.
Li, Z.X., 1998. Tectonic history of the major East Asian lithospheric blocks since the mid-Proterozoic – a synthesis. In: Flower, M.F.J., Chung, S.-L., Lo, C.H., Lee, T.Y. (Eds.), Mantle Dynamics and Plate Interactions in East Asia, American Geophysical Union Geodynamic Series, vol. 27, pp. 221–243.
Li, Z.X., Li, X.H., Kinny, P.D., Wang, J., 1999. The break-up of Rodinia: did it start with a mantle plume beneath South China? Earth and Planetary Science Letters 173, 171–181.
Lin, J.Y., 1985. Spatial and temporal distribution of Emeishan basaltic rocks in three southwestern province (Sichuan, Yun-nan and Guizhou) of China. Chinese Science Bulletin 12, 929–932 (in Chinese).
Lo, C.H., Chung, S.-L., Lee, T.-Y., Wu, G., 2002. Age of the Emeishan flood magmatism and relations to Permian-Triassic boundary events. Earth and Planetary Science Letters 198, 449–458.
Luo, W., Zhang, Z., Hou, T., Wang, M., 2013. Geochronology-geochemistry of the Cida bimodal intrusive complex, central Emeishan large igneous province, southwest China: petrogenesis and plume-lithosphere interaction. International Geology Review 55, 88–114.
Luo, Z.-Y., Xu, Y.-G., He, B., Shi, Y.-R., Huang, X.-L., 2007. Geochronologic and petrochemical evidence for the genetic link between the Maomaogou nepheline syenites and the Emeishan large igneous province. Chinese Science Bulletin 52, 949–958.
Ma, Y.X., Ji, X.T., Li, J.C., Huang, M., Min, Z.Z., 2003. Mineral Resources of Panzhihua, Sichuan Province, SW China. Chengdu University of Technology, 275 pp (in Chinese).
McHone, J.G., 2000. Non-plume magmatism and rifting during the opening of the central Atlantic Ocean. Tectonophysics 316, 287–296.
McKenzie, D., O'Nions, R.K., 1991. Partial melt distributions from inversion of rare earth element concentrations. Journal of Petrology 32, 1021–1091.
Morgan, W.J., 1971. Convection plumes in the lower mantle. Nature 230, 42–43.
Morgan, W.J., 1972. Deep mantle convection plumes and plate motions. The American Association of Petroleum Geologists Bulletin 56, 203–213.
Natland, J.H., Winterer, E.L., 2005. Fissure control on volcanic action in the Pacific. In: Foulger, G.R., Natland, J.H., Presnall, D.C., Anderson, D.L. (Eds.), Plates, Plumes and Paradigms. Geological Society of America, pp. 687–710. Special Paper 388.
Niu, H., Shan, Q., Chen, X., Zhang, H., 2003. Relationship between light rare earth deposits and mantle processes in Panxi rift, China. Science in China 46, 41–49.
Pang, K.-N., Zhou, M.-F., Qi, L., Chung, S.-L., Chu, C.-H., Lee, H.-Y., 2013. Petrology and geochemistry at the LZ-MZa transition of the Panzhihua intrusion: implications for differentiation and oxide ore genesis. Geoscience Frontiers 4, 517–533.
Pang, K.-N., Zhou, M.-F., Qi, L., Shellnutt, J.G., Wang, C.Y., Zhao, D., 2010. Magmatic Fe-Ti-V oxide deposits in the Emeishan large igneous province, SW China. Lithos 119, 123–136.
Pang, K.-N., Li, C., Zhou, M.-F., Ripley, E.M., 2009. Mineral compositional constraints on petrogenesis and oxide ore genesis of the late Permian Panzhihua layered gabbroic intrusion, SW China. Lithos 110, 199–214.
Pang, K.-N., Li, C., Zhou, M.-F., Ripley, E.M., 2008a. Abundant Fe-Ti oxide inclusions in olivine from the Panzhihua and Hongge layered intrusions, SW China: evidence for early saturation of Fe-Ti oxides in ferrobasaltic magma. Contributions to Mineralogy and Petrology 156, 307–321.
Pang, K.-N., Zhou, M.-F., Lindsley, D., Zhao, D., Malpas, J., 2008b. Origin of Fe-Ti oxide ores in mafic intrusions: evidence from the Panzhihua intrusion, SW China. Journal of Petrology 49, 295–313.
Pearce, J.A., Cann, J.R., 1973. Tectonic setting of basic volcanic rocks determined using trace element analyses. Earth and Planetary Science Letters 19, 290–300.
Pearce, J.A., Harris, N.B., Tindle, A.G., 1984. Trace element discrimination diagrams for the tectonic interpretation of granitic rocks. Journal of Petrology 25, 956–983.
Philpotts, A.R., 1982. Compositions of immiscible liquids in volcanic rocks. Contributions to Mineralogy and Petrology 80, 201–218.
Philpotts, A.R., 1976. Silicate liquid immiscibility: it's probable extent and petrogenetic significance. American Journal of Science 276, 1147–1177.
Pilet, S., Hernandez, J., Sylvester, P., Poujol, M., 2005. The metasomatic alternative for ocean island basalt chemical heterogeneity. Earth and Planetary Science Letters 236, 148–166.
Pilet, S., Baker, M.B., Stopler, E.M., 2008. Metasomatized lithosphere and the origin of alkaline lavas. Science 320, 916–919.
Pirajno, F., 2000. Ore Deposits and Mantle Plumes. Kluwer Academic Publishers, Dordrecht, 556 pp.
Plank, T., Langmuir, C.H., 1998. The chemical composition of subducting sediment and its consequences for the crust and mantle. Chemical Geology 145, 325–394.
Polyakov, G.V., Balykin, P.A., Glotov, A.I., Hung, Tran Quoc, Phuong, Ngo Thi, Thanh, Hoang Huu, Nien, Bui An, 1991. Permian-Triassic association of high-magnesian volcanic rocks of the Song Da zone (north-western Vietnam). Soviet Geology and Geophysics 32, 1–11.

Pu, C., Qu, D., Nian, H., Pirajno, F., Fan, Z., 2007. Geological and geochemical characteristics of the Baimazhai Ni-Cu-(PGE) sulphide deposit in Yunnan, China. Chinese Journal of Geochemistry 26, 347–383.
Qi, L., Zhou, M.-F., 2008. Platinum-group elemental and Sr–Nd–Os isotopic geochemistry of Permian Emeishan flood basalts in Guizhou Province, SW China. Chemical Geology 248, 83–103.
Qi, L., Wang, C.Y., Zhou, M.-F., 2008. Controls on the PGE distribution of Permian Emeishan alkaline and peralkaline volcanic rocks in Longzhoushan, Sichuan Province, SW China. Lithos 106, 222–236.
Rainbird, R.H., 1993. The sedimentary record of mantle plume uplift preceding eruption of the Neoproterozoic Natkusiak flood basalt. Journal of Geology 101, 305–318.
Rampino, M.R., Stothers, R.B., 1988. Flood basalt volcanism during the past 250 million years. Science 241, 663–668.
Raup, D.M., Sepkoski, J.J., 1982. Mass extinctions in the marine fossil record. Science 215, 1501–1503.
Renne, P.R., Balco, G., Ludwig, K.R., Mundil, R., Min, K., 2011. Reply to the Comment by W. H. Schwarz et al. on "Joint determination of 40K decay constants and $^{40}Ar^{*}/^{40}K$ for the Fish Canyon sanidine standard, and improved accuracy for $^{40}Ar/^{39}Ar$ geochronology". Geochimica et Cosmochimica Acta 75, 5097–5100.
Renne, P.R., Mundil, R., Balco, G., Min, K., Ludwig, K.R., 2010. Joint determination of 40K decay constants and 40Ar*/40K for the Fish Canyon sanidine standard, and improved accuracy for $^{40}Ar/^{39}Ar$ geochronology. Geochimica et Cosmochimica Acta 74, 5349–5367.
Retallack, G.J., Jahren, A.H., 2008. Methane release from igneous intrusion of coal during Late Permian extinction events. Journal of Geology 116, 1–20.
Richards, M., Duncan, R.A., Courtillot, V.E., 1989. Flood basalts and hotspot tracks: plumes heads and tails. Science 246, 103–107.
Rudnick, R.L., Gao, S., 2003. Composition of the continental crust. In: Rudnick, R.L. (Ed.), The Crust, Treatise on Geochemistry, vol. 3, pp. 1–64.
Salvi, S., Williams-Jones, A.E., 2005. Alkaline granite-syenite deposits. In: Linnen, R.L., Samson, I.M. (Eds.), Rare-element Geochemistry and Mineral Deposits, Geological Association of Canada Short Course Notes, vol. 17, pp. 315–341.
Saunders, A.D., 2005. Large igneous provinces: origin and environmental consequences. Elements 1, 259–263.
Saunders, A.D., Jones, S.M., Morgan, L.A., Pierce, K.L., Widdowson, M., Xu, Y.-G., 2007. Regional uplift associated with continental large igneous provinces: the roles of mantle plume and the lithosphere. Chemical Geology 241, 282–318.
Saunders, A.D., England, R.W., Reichow, M.K., White, R.V., 2005. A mantle plume origin for the Siberian traps: uplift and extension in the west Siberian basin, Russia. Lithos 79, 407–424.
Self, S., Thordarson, T., Widdowson, M., 2005. Gas fluxes from flood basalt eruptions. Elements 1, 283–287.
Shellnutt, J.G., Iizuka, Y., 2013. Chevkinite-group minerals from the mantle derived metaluminous Woshui syenite of the Emeishan large igneous province. European Journal of Mineralogy. http://dx.doi.org/10.1127/0935-1221/2013/0025-2309 (in press).
Shellnutt, J.G., Iizuka, Y., 2012. Oxidation zonation within the Emeishan large igneous province: evidence from mantle-derived syenitic plutons. Journal of Asian Earth Sciences 54-55, 31–40.
Shellnutt, J.G., Iizuka, Y., 2011. Mineralogy from three peralkaline granitic plutons of the Late Permian Emeishan large igneous province (SW China): evidence for contrasting magmatic conditions of A-type granitoids. European Journal of Mineralogy 23, 45–61.
Shellnutt, J.G., Jahn, B.-M., 2011. Origin of Late Permian Emeishan basaltic rocks from the Panxi region (SW China): implications for the Ti-classification and spatial-compositional distribution of the Emeishan basalts. Journal of Volcanology and Geothermal Research 199, 85–95.
Shellnutt, J.G., Jahn, B.-M., 2010. Formation of the Late Permian Panzhihua plutonic-hypabyssal-volcanic igneous complex: implications for the genesis of Fe-Ti oxide deposits and A-type granites of SW China. Earth and Planetary Science Letters 289, 509–519.
Shellnutt, J.G., Pang, K.-N., 2012. Mineral compositions of the Late Permian Baima layered gabbroic intrusion: constraints on petrogenesis. Mineralogy and Petrology 106, 75–88.
Shellnutt, J.G., Denyszyn, S., Mundil, R., 2012a. Precise age determination of mafic and felsic intrusive rocks from the Permian Emeishan large igneous province (SW China). Gondwana Research 22, 118–126.
Shellnutt, J.G., Bhat, G.M., Wang, K.-L., Brookfield, M.E., Dostal, J., Jahn, B.-M., 2012b. Origin of the silicic rocks of the Early Permian Panjal Traps, Kashmir, India. Chemical Geology 334, 154–170.
Shellnutt, J.G., Bhat, G.M., Brookfield, M.E., Jahn, B.-M., 2011a. No link between the Panjal Traps (Kashmir) and the Late Permian mass extinctions. Geophysical Research Letters 38, L19308,. http://dx.doi.org/10.1029/2011GL049032.
Shellnutt, J.G., Wang, K.-L., Zellmer, G.F., Iizuka, Y., Jahn, B.-M., Pang, K.-N., Qi, L., Zhou, M.-F., 2011b. Three Fe-Ti oxide ore-bearing gabbro-granitoid complexes in the Panxi region of the Emeishan large igneous province, SW China. American Journal of Science 311, 773–812.
Shellnutt, J.G., Jahn, B.-M., Zhou, M.-F., 2011c. Crustal-derived granites in the Panzhihua region, SW China: implications for felsic magmatism in the Emeishan large igneous province. Lithos 123, 145–157.
Shellnutt, J.G., Jahn, B.-M., Dostal, J., 2010. Elemental and Sr-Nd isotope geochemistry of microgranular enclaves from peralkaline A-type granitic plutons of the Emeishan large igneous province, SW China. Lithos 119, 34–46.
Shellnutt, J.G., Zhou, M.-F., Zellmer, G., 2009a. The role of Fe–Ti oxide crystallization in the formation of A-type granitoids with implications for the Daly gap: an example from the Permian Baima igneous complex, SW China. Chemical Geology 259, 204–217.
Shellnutt, J.G., Wang, C.Y., Zhou, M.-F., Yang, Y.-H., 2009b. Zircon Lu–Hf isotopic compositions of metaluminous and peralkaline A-type granitic plutons of the Emeishan large igneous province (SW China): constraints on the mantle source. Journal of Asian Earth Sciences 35, 45–55.
Shellnutt, J.G., Zhou, M.-F., Yan, D.-P., Wang, Y., 2008. Longevity of the Permian Emeishan mantle plume (SW China): 1 million years; 8 million years or 18 million years? Geological Magazine 145, 373–388.
Shellnutt, J.G., Zhou, M.-F., 2008. Permian, rifting related fayalite syenite in the Panxi region, SW China. Lithos 101, 54–73.
Shellnutt, J.G., Zhou, M.-F., 2007. Permian peralkaline, peraluminous and metaluminous A-type granites in the Panxi district, SW China: their relationship to the Emeishan mantle plume. Chemical Geology 243, 286–316.
Sheth, H.C., 2007a. 'Large igneous provinces (LIPs)': definition, recommended terminology, and a hierarchial classification. Earth-Sciences Review 85, 117–124.
Sheth, H.C., 2007b. Plume related regional pre-volcanic uplift in the Deccan traps: absence of evidence, evidence of absence. In: Foulger, G.R., Jurdy, D.M. (Eds.), Plates, Plumes and Planetary Processes. Geological Society of America, pp. 785–813. Special Paper 430.
Sheth, H.C., 2005a. Were the Deccan flood basalts derived in part from ancient oceanic crust within the Indian continental lithosphere? Gondwana Research 8, 109–127.
Sheth, H.C., 2005b. From Deccan to Réunion: no trace of a mantle plume. In: Foulger, G.R., Natland, J.H., Presnall, D.C., Anderson, D.L. (Eds.), Plates, Plumes and Paradigms. Geological Society of America, pp. 477–501. Special Paper 388.
Sheth, H.C., 1999. Flood basalts and large igneous province from deep mantle plumes: fact, fiction, and fallacy. Tectonophysics 311, 1–29.
Song, X.-Y., Qi, H.-W., Hu, R.-Z., Chen, L.-M., Yu, S.-Y., Zhang, J.-F., 2013. Formation of thick stratiform Fe-Ti oxide layers in layered intrusion and frequent replenishment of fractionated mafic magma: evidence from the Panzhihua intrusion, SW China. Geochemistry, Geophysics, Geosystems 14, 712–732.
Song, X.-Y., Keays, R.R., Xiao, L., Qi, H.-W., Ihlenfeld, C., 2009. Platinum-group element geochemistry of the continental flood basalts in the central Emeishan large igneous province, SW China. Chemical Geology 262, 246–261.
Song, X.Y., Qi, H.-W., Robinson, P.T., Zhou, M.-F., Cao, Z.-M., Chen, L.-M., 2008a. Melting of the subcontinental lithospheric mantle by the Emeishan mantle plume; evidence from the basal alkaline basalts in Dongchuan, Yunnan, southwestern China. Lithos 100, 93–111.
Song, X.-Y., Zhou, M.-F., Tao, Y., Xiao, J.-F., 2008b. Controls on the metal compositions of magmatic sulfide deposits in the Emeishan large igneous province, SW China. Chemical Geology 253, 38–49.
Song, X.Y., Zhou, M.-F., Keays, R.R., Cao, Z.-M., Sun, M., Qi, L., 2006. Geochemistry of the Emeishan flood basalts at Yangliuping, Sichuan, SW China: implications for sulfide segregation. Contributions to Mineralogy and Petrology 152, 53–74.
Song, X.-Y., Zhong, H., Tao, Y., Zhou, M.-F., 2005. Magmatic sulphide deposits in the Permian Emeishan large igneous province, SW China. In: Mao, J., Bierlein, F.P. (Eds.), Mineral Deposit Research: Meeting the Global Challenge. Proceedings of the Eighth Biennial SGA Meeting, Beijing, pp. 465–467 (Chapter 4–29).
Song, X.-Y., Zhou, M.-F., Cao, Z.-M., Robinson, P., 2004. Late Permian rifting of the South China craton caused by the Emeishan mantle plume? Journal of Geological Society of London 161, 773–781.
Song, X.-Y., Zhou, M.-F., Cao, Z.-M., Sun, M., Wang, Y.-L., 2003. Ni–Cu–(PGE) magmatic sulfide deposits in the Yangliuping area, Permian Emeishan igneous province, SW China. Mineralium Deposita 38, 831–843.
Song, X.-Y., Zhou, M.-F., Hou, Z.-Q., Cao, Z.-M., Wang, Y.-L., Li, Y., 2001. Geochemical constraints on the mantle source of the upper Permian Emeishan continental flood basalts, southwestern China. International Geology Review 43, 213–225.
Sun, S.-s., McDonough, W.F., 1989. Chemical and isotopic systematics of oceanic basalts: implications for mantle composition and processes. In: Saunders, A.D., Norry, M.J. (Eds.), Magmatism in the Ocean Basins. Geological Society of London, pp. 313–435. Special Publication 42.
Sun, X., Wang, S., Sun, W., Shi, G., Sun, Y., Xiong, D., Qu, W., Du, A., 2008. PGE geochemistry and Re-Os of massive sulfide ores from the Baimazhai Cu-Ni deposit, Yunnan province, China. Lithos 105, 12–24.
Sun, Y., Lai, X., Wignall, P.B., Widdowson, M., Ali, J.R., Jiang, H., Wang, W., Yan, C., Bond, D.P.G., Vedrine, S., 2010. Dating the onset and nature of the middle Permian Emeishan large igneous province eruptions in SW China using conodont biostratigraphy and its bearing on mantle plume uplift models. Lithos 119, 20–33.
Tao, Y., Li, C., Hu, R., Qi, L., Qu, W., Du, A., 2010. Re-Os isotopic constraints on the genesis of the Limahe Ni–Cu deposit in the Emeishan large igneous province, SW China. Lithos 119, 137–146.
Tao, Y., Ma, Y., Miao, L., Zhu, F., 2009. SHRIMP U-Pb zircon age of the Jinbaoshan ultramafic intrusion, Yunnan Province, SW China. Chinese Science Bulletin 54, 168–172.
Tao, Y., Li, C., Song, X.-Y., Ripley, E.M., 2008. Mineralogical, petrological, and geochemical studies of the Limahe mafic-ultramafic intrusion and associated Ni-Cu sulfide ores, SW China. Mineralium Deposita 43, 849–872.

Tao, Y., Li, C., Hu, R., Ripley, E.M., Du, A., Zhong, H., 2007. Petrogenesis of the Pt-Pd mineralized Jinbaoshan ultramafic intrusion in the Permian Emeishan large igneous province, SW China. Contributions to Mineralogy and Petrology 153, 321–337.
Thomas, D.N., Rolph, T.C., Shaw, J., Gonzalez de Sherwood, S., Zhuang, Z., 1998. Palaeointensity studies of a Late Permian lava succession from Guizhou Province, South China: implications for post-Kiamen dipole field behavior. Geophysical Journal International 134, 856–866.
Thompson, G.M., Ali, J.R., Song, X.Y., Jolley, D.W., 2001. Emeishan basalts, southwest China: reappraisal of the formation's type area stratigraphy and a discussion of its significance as a large igneous province. Journal of the Geological Society of London 158, 593–599.
Utskins-Peate, I., Bryan, S.E., Wignall, P.B., Jerram, D.A., Ali, J.R., 2011. Comment on 'Paleokarst on the top of the Maokou Formation: further evidence for domal crustal uplift prior to the Emeishan flood volcanism'. Lithos 125, 1006–1008.
Utskins-Peate, I., Bryan, S.E., 2009. Reply to pre-eruptive uplift in the Emeishan. Nature Geoscience 2, 531–532.
Utskins-Peate, I., Bryan, S.E., 2008. Re-evaluating plume induced uplift in the Emeishan large igneous province. Nature Geoscience 1, 625–629.
van Olphen, H., 1959. Ion adsorption on clays: a review. Clay and Clay Minerals 8, 115.
Veksler, I.V., Dorfman, A.M., Borisov, A.A., Wirth, R., Dingwell, D., 2007. Liquid immiscibility and the evolution of basaltic magma. Journal of Petrology 48, 2187–2210.
Veksler, I.V., Dorfman, A.M., Danyushevsky, L.V., Jakobsen, J.K., Dingwell, D.B., 2006. Immiscible silicate liquid partition coefficients: implications for crystal-melt element partitioning and basalt petrogenesis. Contributions to Mineralogy and Petrology 152, 685–702.
Wang, H., Mo, X., 1995. An outline of the tectonic evolution of China. Episodes 18, 6–16.
Wang, C.Y., Zhou, M.-F., Qi, L., 2011. Chalcophile element geochemistry and petrogenesis of high-Ti and low-Ti magmas in the Permian Emeishan large igneous province, SW China. Contributions to Mineralogy and Petrology 161, 237–254.
Wang, C.Y., Zhou, M.-F., Qi, L., 2010. Origin of extremely PGE-rich mafic magma system: an example from the Jinbaoshan ultramafic sill, Emeishan large igneous province, SW China. Lithos 119, 147–161.
Wang, C.Y., Zhou, M.-F., Zhao, D., 2008a. Fe-Ti-Cr oxides from the Permian Xinjie mafic-ultramafic layered intrusion in the Emeishan large igneous province, SW China: crystallization from Fe- and Ti-rich basaltic magmas. Lithos 102, 198–217.
Wang, C.Y., Prichard, H.M., Zhou, M.-F., Fisher, P.C., 2008b. Platinum-group minerals from the Jinbaoshan Pd-Pt deposit, SW China: evidence for magmatic origin and hydrothermal alteration. Mineralium Deposita 43, 791–803.
Wang, C.Y., Zhou, M.-F., Qi, L., 2007. Permian flood basalts and mafic intrusions in the Jinping (SW China)–Song Da (northern Vietnam) district: mantle sources, crustal contamination and sulfide segregation. Chemical Geology 243, 317–343.
Wang, C.Y., Zhou, M.-F., Keays, R.R., 2006a. Geochemical constraints on the origin of the Permian Baimazhai mafic–ultramafic intrusion, SW China. Contributions to Mineralogy and Petrology 152, 309–321.
Wang, C.Y., Zhou, M.-F., Qi, L., Hou, S., Gao, H., 2006b. The Zhangtong native copper deposit associated with the Permian Emeishan flood basalts, Yunnan, Southwest China. International Geology Review 48, 742–768.
Wang, C.Y., Zhou, M.-F., 2006. Genesis of the Permian Baimazhai magmatic Ni-Cu-(PGE) sulfide deposit, Yunnan, SW China. Mineralium Deposita 41, 771–783.
Wang, C.Y., Zhou, M.-F., Zhao, D.G., 2005. Mineral chemistry of chromite from the Permian Jinbaoshan Pt-Pd-sulphide-bearing ultramafic intrusion in SW China with petrogenetic implications. Lithos 83, 47–66.
Watson, E.B., 1976. Two-liquid partition coefficients: experimental data and geochemical implications. Contributions to Mineralogy and Petrology 56, 119–134.
White, R.V., 2002. Earth's biggest 'whodunnit': unraveling the clues in the case of the end-Permian mass extinction. Philosophical Transactions of the Royal Society, London A 360, 2963–2985.
White, R.V., Saunders, A.D., 2005. Volcanism, impact and mass extinctions: incredible or coincidence? Lithos 79, 299–316.
White, R.S., McKenzie, D., 1995. Mantle plumes and flood basalts. Journal of Geophysical Research 100, 543–585.
White, R.S., McKenzie, D., 1989. Magmatism at rift zones: the generation of volcanic continental margins and flood basalts. Journal of Geophysical Research 94, 7685–7729.
Wilson, J.T., 1963. Hypothesis of Earth's behavior. Nature 198, 925–929.
Wilson, M., 1989. Igneous Petrogenesis: a Global Tectonic Approach. Unwin Hyman Ltd., London, p. 466.
Winchester, J.A., Floyd, P.A., 1977. Geochemical discrimination of different magma series and their differentiation products using immobile elements. Chemical Geology 20, 325–343.
Wignall, P., 2005. The link between large igneous province eruptions and mass extinctions. Elements 1, 293–297.
Wignall, P., 2001. Large igneous provinces and mass extinctions. Earth Science Reviews 53, 1–33.
Wignall, P.B., Sun, Y., Bond, D.P.G., Izon, G., Newton, R.J., Vedrine, S., Widdowson, M., Ali, J.R., Lai, X., Jiang, H., Cope, H., Bottrell, S.H., 2009. Volcanism, mass extinction, and carbon isotope fluctuations in the middle Permian of China. Science 324, 1179–1182.
Xiao, L., Xu, Y.G., Mei, H.J., Zheng, Y.F., He, B., Pirajno, F., 2004. Distinct mantle sources of low-Ti and high-Ti basalts from the western Emeishan large igneous province, SW China: implications for plume–lithosphere interaction. Earth and Planetary Science Letters 228, 525–546.
Xiao, L., Xu, Y.-G., Chung, S.-L., He, B., Mei, H., 2003. Chemostratigraphic correlation of upper Permian lavas from Yunnan Province, China: extent of the Emeishan large igneous province. International Geology Review 45, 753–766.
Xu, C., Taylor, R.N., Li, W., Kynicky, J., Chakhmouradian, A.R., Song, W., 2012. Comparison of fluorite geochemistry from REE deposits in the Panxi region and Bayan Oba, China. Journal of Asian Earth Sciences 57, 76–89.
Xu, J.-F., Suzuki, K., Xu, Y.-G., Mei, H.-J., Li, J., 2007. Os, Pb, and Nd isotope geochemistry of the Permian Emeishan continental flood basalts: insights into the source of a large igneous province. Geochimica et Cosmochimica Acta 71, 2104–2119.
Xu, Y.-G., He, B., 2007. Thick and high velocity crust in Emeishan large igneous province, SW China: evidence for crustal growth by magmatic underplating/intraplating. In: Foulger, G.R., Jurdy, D.M. (Eds.), Plates, Plumes and Planetary Processes. Geological Society of America, pp. 841–858. Special Paper 430.
Xu, Y.-G., Chung, S.-L., Chung, Shao, H., He, B., 2010. Silicic magmas form the Emeishan large igneous province, southwest China: petrogenesis and their link with the end-Guadalupian biological crisis. Lithos 119, 47–60.
Xu, Y.-G., Luo, Z.-Y., Huang, X.-L., He, B., Xiao, L., Xie, L.-W., Shi, Y.-R., 2008. Zircon U-Pb and Hf isotope constraints on crustal melting associated with the Emeishan mantle plume. Geochimica et Cosmochimica Acta 72, 3084–3104.
Xu, Y.-G., He, B., Huang, X., Luo, Z., Zhu, D., Ma, J., Shao, H., 2007a. Late Permian Emeishan flood basalts in southwestern China. Earth Science Frontiers 14, 1–9.
Xu, Y.-G., He, B., Huang, X., Luo, Z., Chung, S.-L., Xiao, L., Zhu, D., Shao, Fan, W.-M., Xu, J., Wang, Y.-J., 2007b. Identification of mantle plumes in the Emeishan large igneous province. Episodes 30, 32–42.
Xu, Y.G., He, B., Chung, S.L., Menzies, M., Frey, F.A., 2004. Geologic, geochemical, and geophysical consequences of plume involvement in the Emeishan flood-basalt province. Geology 32, 917–920.
Xu, Y., Mei, H., Xu, J., Huang, X., Wang, Y., Chung, S.-L., 2003. Origin of two differentiation trends in the Emeishan flood basalts. Chinese Science Bulletin 48, 390–394.
Xu, Y., Chung, S.L., Jahn, B.-M., Wu, G., 2001. Petrologic and geochemical constraints on the petrogenesis of Permian-Triassic Emeishan flood basalts in southwestern China. Lithos 58, 145–168.
Yan, D.-P., Zhou, M.-F., Wang, C.Y., Xia, B., 2006. Structural and geochronological constraints on the tectonic evolution of the Dulong-Song Chay tectonic dome in Yunnan province, SW China. Journal of Asian Earth Sciences 28, 332–353.
Yan, D.P., Zhou, M.-F., Song, H.L., Wang, X.W., Malpas, J., 2003. Origin and tectonic significance of a mesozoic multi-layer over-thrust system within the Yangtze Block (South China). Tectonophysics 361, 239–254.
Yin, A., Harrison, T.M., 2000. Geological evolution of the Himalayan-Tibetan orogen. Annual Reviews in Earth and Planetary Science 28, 211–280.
Zhang, M., O'Reilly, S.Y., Wang, K.-L., Hronsky, J., Griffin, W.L., 2008a. Flood basalts and metallogeny: the lithospheric mantle connection. Earth-science Reviews 86, 145–174.
Zhang, Y.X., Luo, Y., Yang, X., 1988. The Panxi Rift. Geological Press, Beijing (in Chinese).
Zhang, Z., Mao, J., Saunders, A.D., Ai, Y., Li, Y., Zhao, L., 2009. Petrogenetic modeling of three mafic-ultramafic layered intrusions in the Emeishan large igneous province, SW China, based on isotopic and bulk chemical constraints. Lithos 113, 369–392.
Zhang, Z., Zhi, X., Chen, L., Saunders, A.D., Reichow, M.K., 2008b. Re-Os isotopic compositions of picrites from the Emeishan flood basalt province, China. Earth and Planetary Science Letters 276, 30–39.
Zhang, Z., Mahoney, J.J., Mao, J., Wang, F., 2006a. Geochemistry of picritic and associated basalt flows of the western Emeishan flood basalt province, China. Journal of Petrology 47, 1997–2019.
Zhang, Z., Mao, J., Wang, F., Pirajno, F., 2006b. Native gold and native copper grains enclosed by olivine phenocrysts in a picritic lava of the Emeishan large igneous province, SW China. American Mineralogist 91, 1178–1183.
Zhang, Z., Mao, J., Wang, F., Hao, Y., Mahoney, J.J., 2005. Mantle plume activity and melting conditions: evidence from olivines in picritic-komatiitic rocks from the Emeishan large igneous province, southwestern China. Episodes 28, 171–176.
Zhao, J.-H., Zhou, M.-F., 2007. Geochemistry of Neoproterozoic mafic intrusions in the Panzhihua district (Sichuan Province, SW China): implications for subduction-related metasomatism in the upper mantle. Precambrian Research 152, 27–47.
Zhao, G., Sun, M., Wilde, S.A., Li, S., Zhang, Jian, 2006. Some key issues in reconstructions of proterozoic supercontinents. Journal of Asian Earth Sciences 28, 3–19.
Zhao, G., Sun, M., Wilde, S.A., Li, S., 2005. Late Archean to Paleoproterozoic evolution of the North China Craton: key issues revisited. Precambrian Research 136, 177–202.
Zheng, L., Yang, Z., Tong, Y., Yuan, W., 2010. Magnetostratigraphic constraints on two-stage eruptions of the Emeishan continental flood basalts. Geochemistry, Geophysics, Geosystems 11, Q12014. http://dx.doi.org/10.1029/2010GC003267.
Zhong, H., Zhu, W.-G., 2006. Geochronology of layered mafic intrusions from the Pan-Xi area in the Emeishan large igneous province, SW China. Mineralium Deposita 41, 599–606.
Zhong, H., Qi, L., Hu, R.-Z., Zhou, M.-F., Gou, T.-Z., Zhu, W.-G., Liu, B.-G., Chu, Z.-Y., 2011a. Timing and source constraints on the relationship between mafic and felsic intrusions in the Emeishan large igneous province. Geochimica et Cosmochimica Acta 75, 1374–1395.

Zhong, H., Qi, L., Hu, R.-Z., Zhou, M.-F., Gou, T.-Z., Zhu, W.-G., Liu, B.-G., Chu, Z.-Y., 2011b. Rhenium-osmium isotope and platinum-group elements in the Xinjie layered intrusion, SW China: implications for source mantle composition, mantle evolution, PGE fractionation and mineralization. Geochimica et Cosmochimica Acta 75, 1621–1641.

Zhong, H., Zhu, W.-G., Hu, R.-Z., Xie, L.-W., He, D.-F., Liu, F., Chu, Z.-Y., 2009. Zircon U-Pb age and Sr-Nd-Hf isotope geochemistry of the Panzhihua A-type syenitic intrusion in the Emeishan large igneous province, southwest China and implications for growth of juvenile crust. Lithos 110, 109–128.

Zhong, H., Hu, R.-Z., Wilson, A.H., Zhu, W.-G., 2005. Review of the link between the Hongge layered intrusion and Emeishan flood basalts, southwest China. International Geology Review 47, 971–985.

Zhong, H., Yao, Y., Prevec, S.A., Wilson, A.H., Viljoen, M.J., Viljoen, R.P., Liu, B.-G., Luo, Y.-N., 2004. Trace-element and Sr-Nd isotopic geochemistry of the PGE-bearing Xinjie layered intrusion in SW China. Chemical Geology 203, 237–252.

Zhong, H., Yao, Y., Hu, S.F., Zhou, X.H., Liu, B.G., Sun, M., Zhou, M.-F., Viljoen, M.J., 2003. Trace-element and Sr-Nd isotopic geochemistry of the PGE-bearing Hongge layered intrusion, southwestern China. International Geology Review 45, 371–382.

Zhong, H., Zhu, W.-G., Song, X.-Y., He, D.-F., 2007. SHRIMP U-Pb zircon geochronology, geochemistry, and Nd-Sr isotopic study of contrasting granites in the Emeishan large igneous province, SW China. Chemical Geology 236, 112–137.

Zhong, H., Zhou, X.H., Zhou, M.-F., Sun, M., Liu, B.G., 2002. Platinum-group element geochemistry of the Hongge Fe-V-Ti deposit in the Pan-Xi area, southwestern China. Mineralium Deposita 37, 226–239.

Zhou, M.-F., Chen, W.T., Wang, C.Y., Prevec, S.A., Liu, P.P., Howarth, G.H., 2013. Two stages of immiscible liquid separation in the formation of Panzhihua-type Fe-Ti-V oxide deposits, SW China. Geoscience Frontiers 4, 481–502.

Zhou, M.-F., Arndt, N.T., Malpas, J., Wang, C.Y., Kennedy, A.K., 2008. Two magma series and associated ore deposit types in the Permian Emeishan large igneous province, SW China. Lithos 103, 352–368.

Zhou, M.-F., Zhao, J.-H., Qi, L., Su, W., Hu, R.Z., 2006. Zircon U-Pb geochronology and elemental and Sr -Nd isotopic geochemistry of Permian mafic rocks in the Funing area, SW China. Contributions to Mineralogy and Petrology 151, 1–19.

Zhou, M.-F., Robinson, P.T., Lesher, C.M., Keays, R.R., Zhang, C.J., Malpas, J., 2005. Geochemistry, petrogenesis and metallogenesis of the Panzhihua gabbroic layered intrusion and associated Fe-Ti-V oxide deposits, Sichuan Province, SW China. Journal of Petrology 46, 2253–2280.

Zhou, M.-F., Malpas, J., Song, X.-Y., Robinson, P.T., Sun, M., Kennedy, A.K., Lesher, C.M., Keays, R.R., 2002a. A temporal link between the Emeishan large igneous province (SW China) and the end-Guadalupian mass extinction. Earth and Planetary Science Letters 196, 113–122.

Zhou, M.-F., Yan, D.P., Kennedy, A.K., Li, Y., Ding, J., 2002b. SHRIMP U-Pb zircon geochronological and geochemical evidence for Neoproterozoic arc-magmatism along the western margin of the Yangtze block, South China. Earth and Planetary Science Letters 196, 51–67.

Zhu, B.-Q., Hu, Y.-G., Zhang, Z.-W., Cui, X.-J., Dai, T.-M., Chen, G.-H., Peng, J.-H., Sun, Y.-G., Liu, D.-H., Chang, X.-Y., 2007. Geochemistry and geochronology of native copper mineralization related to the Emeishan flood basalts, Yunnan Province, China. Ore Geology Reviews 32, 366–380.

Zhu, D., Luo, T.-Y., Gao, Z.-M., 2003. Differentiation of the Emeishan Flood Basalts at the Base and throughout the Crust of Southwest China. International Geology Review 45, 471–477.

Zhu, W.-G., Zhong, H., Hu, R.-Z., Liu, B.-G., He, D.-F., Song, X.-Y., Deng, H.-L., 2010. Platinum-group minerals and tellurides from the PGE-bearing Xinjie layered intrusion in the Emeishan large igneous province, SW China. Mineralogy and Petrology 98, 167–180.

Zindler, A., Hart, S.R., 1986. Chemical geodynamics. Annual Review of Earth and Planetary Sciences 14, 493–571.

Dr J. Gregory Shellnutt is an Assistant Professor at National Taiwan Normal University (NTNU) in Taipei. He received his Ph.D. from The University of Hong Kong (2007), which focused on the formation of A-type granites within the Emeishan large igneous province and their association with the giant Fe-T-V oxide-ore bearing gabbroic intrusions. As a post-doctoral researcher at Academia Sinica (Taipei) he continued his work large igneous provinces and granite petrogenesis. He now manages the new wavelength-dispersive X-ray Fluorescence laboratory (WD-XRF) at NTNU mainly conducting whole rock analyses for the geosciences community in Taiwan. His personal research interests are on the formation of alkaline granitic rocks on Earth and Venus, the formation of orthomagmatic Fe-Ti-V oxide deposits, giant radiating mafic dyke swarms and origin of orogenic peridotites within accretionary terranes.